

ECOLE POLYTECHNIQUE
PROMOTION X2000
SPIGA Aymeric
aymeric.spiga@polytechnique.org

Rapport de stage d'option

Paleoclimatology of Planet Mars :
Simulation and Analysis of Mars climate and
water cycle at High Obliquity

NON CONFIDENTIEL

Département de Mécanique
Océan et environnement

Directeur de l'option : Hervé Le Treut
Directeur de Stage : Robert M. Haberle

Date du Stage : 21 Avril-19 Juillet 2003
Lieu du Stage :

Space science Division
NASA Ames Research Center
Moffet Field
CA 94035-1000
USA

Abstract

My Ecole Polytechnique internship consisted in working on improved simulations of Mars climate, with a higher obliquity than the present-day planet. I worked three months with the Mars General Circulation Model (MGCM) team, led by Robert M. Haberle, in NASA Ames Research Center, California.

Several simulations of Mars climate have been made at high obliquity - and have produced a great deal of interesting results. Nevertheless, these previous simulations did not include enough reasonable physics to be totally relevant. It is worth saying that since these first numerical experiments at high obliquity, several breakthroughs have been made in simulating Mars clouds and water cycle. Furthermore, the MGCM have been improved, especially its ability to reproduce radiative transfers.

My work has benefited of all these progresses. It consisted in start new simulations, analyze the results, in order to start figuring out what could have been Mars climate and water cycle, few thousands years ago, when the obliquity could have been higher than it is presently.

Resumé

Le stage d'option de l'Ecole Polytechnique a été pour moi l'occasion de travailler sur des simulations améliorées du climat de Mars à haute obliquité. Ce stage, long de trois mois, s'est déroulé au sein de l'équipe du Mars General Circulation Model (MGCM), dirigée par Robert M. Haberle, au Centre de Recherches de NASA Ames, en Californie.

Ce n'est pas la première fois que des simulations sont lancées en modélisant Mars à haute obliquité. Les résultats obtenus étaient intéressants, même si la physique utilisée péchait quelque peu par manque de réalisme. D'où l'intérêt d'inclure à ces premières expériences les progrès réalisés en matière de simulation des nuages et du cycle de l'eau sur Mars. De plus, le MGCM a subi depuis des améliorations conséquentes, notamment dans la modélisation des transferts radiatifs.

Mon travail a bénéficié de ces multiples progrès. Pendant mon stage, j'ai ainsi été en mesure de lancer de nouvelles simulations, d'analyser les résultats, afin d'ébaucher une description aussi fine que possible du climat martien tel qu'il a pu être il y a plusieurs milliers d'années de cela, lorsque l'obliquité de la planète était probablement plus grande qu'à l'heure actuelle.

Contents

Introduction	4
1 An overview of the present-day Mars atmosphere and climate	5
1.1 General facts	5
1.1.1 Comparative arguments	5
1.1.2 First remarks about the climate	5
1.1.3 Topography	7
1.2 A closer look to the climate of Mars	7
1.2.1 Vertical Structure	8
1.2.2 General circulation	8
1.2.3 Cycles	9
1.3 Radiative influence of atmospheric components	14
1.3.1 CO_2	14
1.3.2 Dust	14
1.3.3 H_2O and other radiative components	14
2 Background and preliminary analysis of the high-obliquity Mars paleo-climate	16
2.1 Basic facts about paleo-climates	16
2.1.1 Climate changes throughout ages	16
2.1.2 Obliquity variations	16
2.2 The Ames Mars General Circulation model	19
2.2.1 Introduction to the model	19
2.2.2 Simulations done	20
2.3 Quasi-periodic climate changes : an overview with a preliminary analysis of simulations	21
2.3.1 Ground temperature	21
2.3.2 Volatile cycles	21
3 Water cycle in high-obliquity Mars	25
3.1 Main simulation : 60° obliquity case	25
3.1.1 Water vapor	25
3.1.2 Ice clouds	25
3.1.3 Ground ice	26
3.1.4 General circulation	29
3.1.5 Conclusion for Mars at 60° obliquity	29
3.2 Comparative simulations : 35° and 45° obliquity cases	30
3.2.1 Water cycle	30
3.2.2 Ground ice location	30
3.2.3 General circulation	32
3.2.4 Conclusion of the comparative study	34

4 Simulations including the H_2O radiative effect	35
4.1 1D preliminary simulations	35
4.2 Atmospheric behavior	37
4.3 Water cycle behaviour	38
4.4 Conclusion	40
5 Conclusions : Abstract	42
Bibliography	46

Introduction

Mars is the most studied planet of our Solar System. There are many reasons for that, including the fact that scientists used to wonder if there was life, liquid water, or oxygen on Mars. Our knowledge, since these times of nearly metaphysical speculations, has been dramatically improved, mostly because of the missions launched to the Red planet.

Mars is still a high-priority target for exploration, atmospheric science, geology, exo-biology. For example, during our internship, the European Space Agency launched the Mars Express mission, while the NASA launched the Mars Exploration Rover. Let us emphasize the point that atmospheric science is one of the key objective of many of the missions being launched.

We wish to end this short introduction recalling that the more we learn about Mars' climate and its origin, the more we learn about Earth's climate and origin. Consequently, the results and the problematics about Mars are widely useful.

Chapter 1

An overview of the present-day Mars atmosphere and climate

1.1 General facts

1.1.1 Comparative arguments

As pointed out by figure 1.1, the present atmosphere of Mars shows a lot of similarity with Earth's (orbital parameters, atmospheric characteristics). This is why we know the Mars' climate will not be very different from Earth's. Even great differences are quite well compensated, for example, we note a relative weakness of gravity on Mars, but this effect is compensated by the denser composition of the atmosphere. Consequently, the thermodynamical characteristic height is quite similar for the two planets.

Of course, there are also important differences [6]. The Martian atmosphere is primarily made of carbon dioxide (partial pressure for carbon dioxide 30 times higher than on Earth) with a much lower surface temperature than Earth's. Present-Day Mars does not possess oceans and its atmosphere is very dry. It does, however, contain suspended dust particules, which radiative role is predominant (see below). The ground pressure is 100 times smaller on Mars (the global annually averaged surface pressure is 6.1HPa), so we will not be surprised to find a weak greenhouse effect compared to Earth.

1.1.2 First remarks about the climate

Mars' atmosphere is thin and relatively transparent to sunlight. Consequently, temperature depends critically on Mars' orbital parameters. The main points are that :

1. Mars receives about half as much annually averaged sunlight as Earth
2. its orbit is much more eccentric than Earth's
3. its rotation rate and obliquity are similar to Earth's

Consequently, Mars is colder, experiences a much greater seasonal change of insolation (40% compared to 6% on Earth), has Earthlike diurnal and seasonal changes, and has a similar Coriolis parameter.

As on Earth, the general circulation is also fundamentally driven by solar heating. However, because of the short radiative response time of Mars' atmosphere (the surface is never far from the radiative equilibrium), the low thermal inertia of the material covering its surface (Mars lacks oceans), and the characteristics of the orbital parameters seen below, the diabatic forcing and the circulation it drives vary significantly on diurnal, monthly, seasonal and interannual time scales [18]. These changes are substantially greater than those in the ocean-buffered troposphere of the Earth. If we would like to compare the two climates, we would describe Mars' climate as "ultra-continental".

Parameters	units	Mars	Earth
Orbital parameters			
Planetary radius a	km	3397	6369
Gravity g	$m.s^{-2}$	3.73	9.81
Sun-planet distance	UA	1.38-1.67	0.98-1.02
Orbital eccentricity		0.0934	0.0167
Obliquity	deg.	25.2	23.98
Solar day (sol)	s	88775	86400
Planetary rotation rate	$10^{-4}s$	0.709	0.729
Year length	sols	669	365
Atmosphere components			
Carbon dioxide CO_2	% per volume	95.3	0.03
Nitrogen N_2	"	2.7	78.1
Argon Ar	"	1.6	0.93
Oxygen O_2	"	0.13	20.9
Carbon monoxide CO	"	0.07	7.10^{-6}
Water vapor H_2O	"	0.03	1
Atmosphere thermodynamics			
Mean molecular weight	$g.mol^{-1}$	43.49	27.8
Molecular gas constant (R)	$m^2.s^{-2}.K^{-1}$	191	287
Specific heat at constant p (c_p)	$J.K^{-1}.kg^{-1}$	0.257	0.2857
Pressure at ref. level altitude	hPa	5 - 8	1013
Planet equilibrium temperature	K	210	256
Thermodynamical characteristic height (H)	km	10	7.8

Figure 1.1: Planetary constants for Mars and Earth [2, 18]

The globally averaged surface temperature on Mars is approximately 215 K. The lowest surface temperatures (approx 150 K) occur in polar regions during winter and are associated with the condensation of CO_2 onto the surface. The highest surface temperature (approx 300 K) occur in the southern subtropics when Mars is closest to the Sun. In these same regions, diurnal variations can exceed 100 K.

1.1.3 Topography

With Mars Orbiter Laser Altimeter (MOLA), Mars' topography (see figure 1.2) is perhaps as precisely known as Earth's. The topography of Mars is a bit more irregular than Earth's : mountains are higher and craters are deeper. The main mountains are the Tharsis volcanos (0° lat, -120° lon), Olympus Mons (20° lat, -130° lon), and Alba Patera plateau (45° lat, -120° lon). The Hellas crater (-50° lat, 60° lon) gives a good example of the contrasts in Martian topography. It is worth mentioning the long canyon at the equator between longitude 100° , and -30° , Valles Marineris. This crustal fissure is a reminiscence of the Tharsis' formation period.

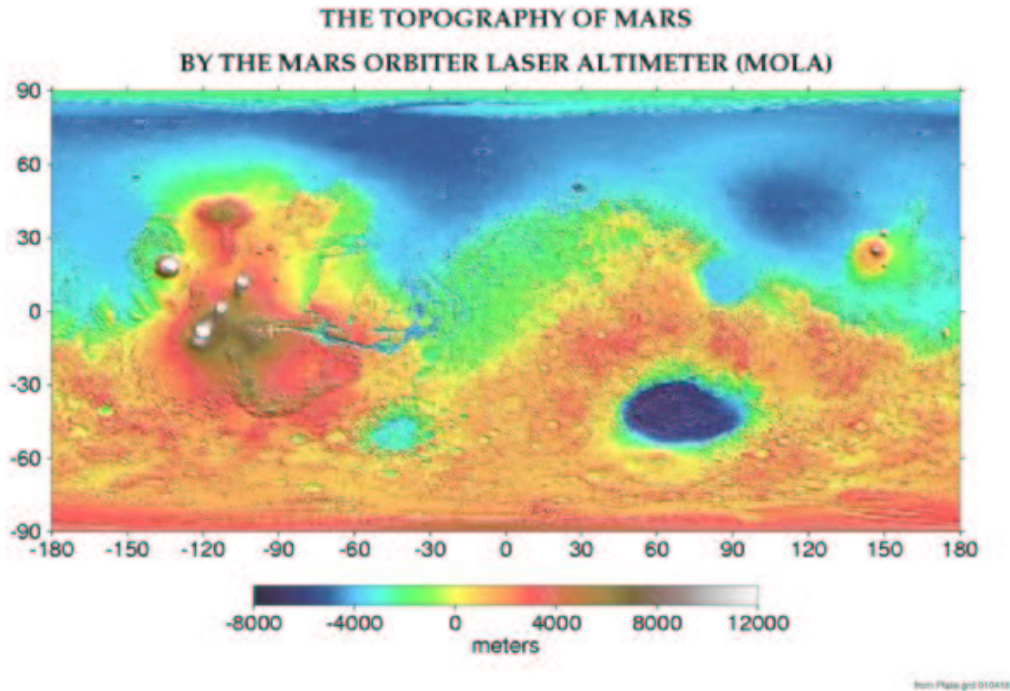


Figure 1.2: Topography Map

1.2 A closer look to the climate of Mars

On Mars, seasons are conventionnally expressed in terms of L_s , the aerocentric longitude of the Sun. This is a an angular measure (in degree) of the apparent revolution of the Sun about Mars. L_s is measured from the intersection of Mars' equatorial plane with the plane of its orbit (the vernal equinox). Consequently, $L_s = 0^\circ$ corresponds to the Northern spring equinox (see figure 1.3).

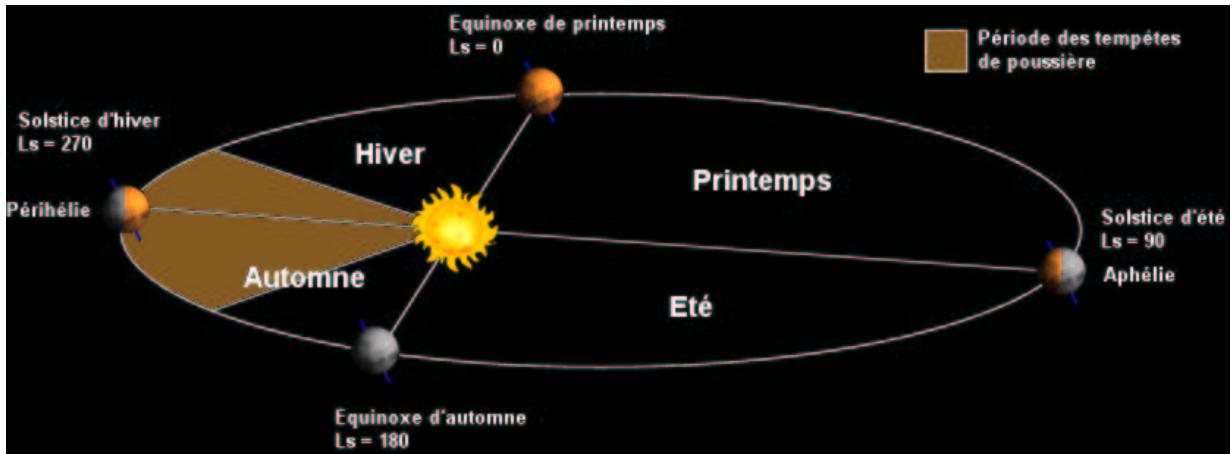


Figure 1.3: Seasons on Mars

1.2.1 Vertical Structure

Temperatures decrease with height in the Martian atmosphere as they do on Earth. The variation of temperature gives rise to a troposphere, a mesosphere, and a thermosphere. Mars does not have a stratosphere, because it lacks an ozone layer.

The troposphere of Mars is deep by comparison to Earth. Based on *Viking* and *Pathfinder* lander entry measurements, the troposphere on Mars extends to almost 60 km with an average lapse rate of 2.5 K.km^{-1} . On Earth, the troposphere is about 12 km deep, and the lapse rate is 6.5 K.km^{-1} .

In Earth's troposphere, evaporation and condensation of water are powerful means of redistributing heat. On Mars, as in the Earth's stratosphere, there is too little atmospheric water for its latent heat to be significant thermodynamically. However, a strong heating comes from the absorption of solar radiation by dust particles, blown into the atmosphere by strong winds at the surface of Mars. This provides a powerful internal heat source somewhat analogous to the latent heat of condensed water in Earth's troposphere. Finally, on both planets, temperature are further stabilized by vertical heat fluxes associated with large-scale circulation systems.

Theoretical studies indicate that daytime boundary layer convection could extend to very high altitudes on Mars, 15 km. Above 15 km, temperatures continue to decrease with height, but are controlled almost entirely by radiation rather than convection.

In the martian mesosphere, we should mention that temperatures become nearly constant, due to a complex role played by "planetary waves", associated with a global system of thermal tides. Finally, in the thermosphere, temperatures increase because of heating due to the absorption of solar radiation in the far and extreme UV part of the spectrum. This also occurs on Earth. The base of the thermosphere is about 80 km on Earth, and about 100 km on Mars.

1.2.2 General circulation

The mechanisms by which momentum, heat, trace gases and aerosols are transported across the planet are still not fully characterized for Mars. Zonally symmetric circulations appear to be more important components of the Martian circulations. In some sense, the Hadley circulation on Earth, a zonal-mean overturning cell with rising air at low latitudes and sinking motion in the subtropics, exists only in the climatological or averaged sense (see [12], chapter 7, which also features a simple calculation of the Mars case). Dynamical theory and the observation of atmospheric temperatures and of surface winds streaks suggest that on Mars there is a more physically coherent, zonally symmetric Hadley cell [3, 18]. This reflects both the strong radiative heating of the dusty Martian atmosphere and, unlike Earth, the seasonal condensation and sublimation on Mars of the significant fraction of the total atmospheric mass. On Mars, atmospheric pressure gradients quickly arise in response to

this mass loss or gain to drive motions (the "condensation/sublimation wind") that transport CO_2 as needed between the two polar regions.

Let us summarize the conclusions of Haberle *et al.*, in their 1993 article [4], about the seasonal behavior of the main large-scale components of the general circulation ¹:

- At the equinoxes (around $Ls = 0^\circ$ or 180°), two Earth-like roughly symmetric Hadley cells develop that share a common rising branch centered at or near the equator, with westerly winds in the mid-latitudes of each hemisphere, and easterlies in the tropics.
- At the solstices (around $Ls = 90^\circ$ or 270°), the two Hadley cells give way to a single-cross equatorial circulation. Westerlies dominate the winter hemisphere, while easterlies dominate the summer hemisphere.
- Models indicate that the intensity of the Hadley cell mass flux varies from $10^9 kg.s^{-1}$ at the equinoxes to $10^{10} kg.s^{-1}$ at the solstices. The simulated zonal winds are about half as strong as they are at solstice. With increasing amounts of dust (up to $\tau = 5$), the zonal mean circulation at northern winter solstice intensifies.

The general circulation process features also phenomena like baroclinic waves and storm systems, Kelvin waves, tides, and more complex winds. Our presentation has no pretention to be exhaustive.

Let us have a look now at the seasonal cycles of carbon dioxide, water and dust, which characterize the climate of Mars. Each of these cycles involves the exchange of material between surface and atmospheric reservoirs. The exchange itself is driven by daily and seasonal variations in insolation. The atmosphere plays a major role in these cycles by serving - as seen in this subsection - as the agent of transport.

1.2.3 Cycles

CO_2

During winter, temperatures in the polar regions become low enough for CO_2 to condense. The condensation of CO_2 during winter and its subsequent sublimation during spring give rise to the familiar waxing and waning of the polar caps. Approximately 20% of the Martian atmosphere is cycled into and out of the polar regions each year by this process.

The waxing and waning of the polar caps leads to a pronounced semiannual variation in the daily averaged surface pressure. The variation is semiannual rather than annual because while one cap is growing the other cap is retreating. However, the variation is asymmetric, with a much deeper minimum occurring during southern winter than during northern winter. This asymmetry is a direct consequence of Mars' orbital eccentricity. Southern winters are longer than northern winters, so that much more CO_2 condenses out of the atmosphere. As a result, pressures are lowest during the middle of southern winter, and highest in late spring when the cap has disappeared.

At both poles, however, the caps never completely disappear during summer (a fact that will not be true at higher obliquity). At the north pole the seasonal CO_2 frost deposit completely sublimates by summer, and exposes an underlying water ice cap. At the south pole, CO_2 frost appears to survive all summer long. Thus, the summer caps have different compositions. The reason for this compositional asymmetry is not understood.

H_2O

Thermodynamics

We take advantage of this section specially dedicated to the water cycle to remember several thermodynamical facts about water on Mars.

¹Precisions can be also found in Forget et al [3]

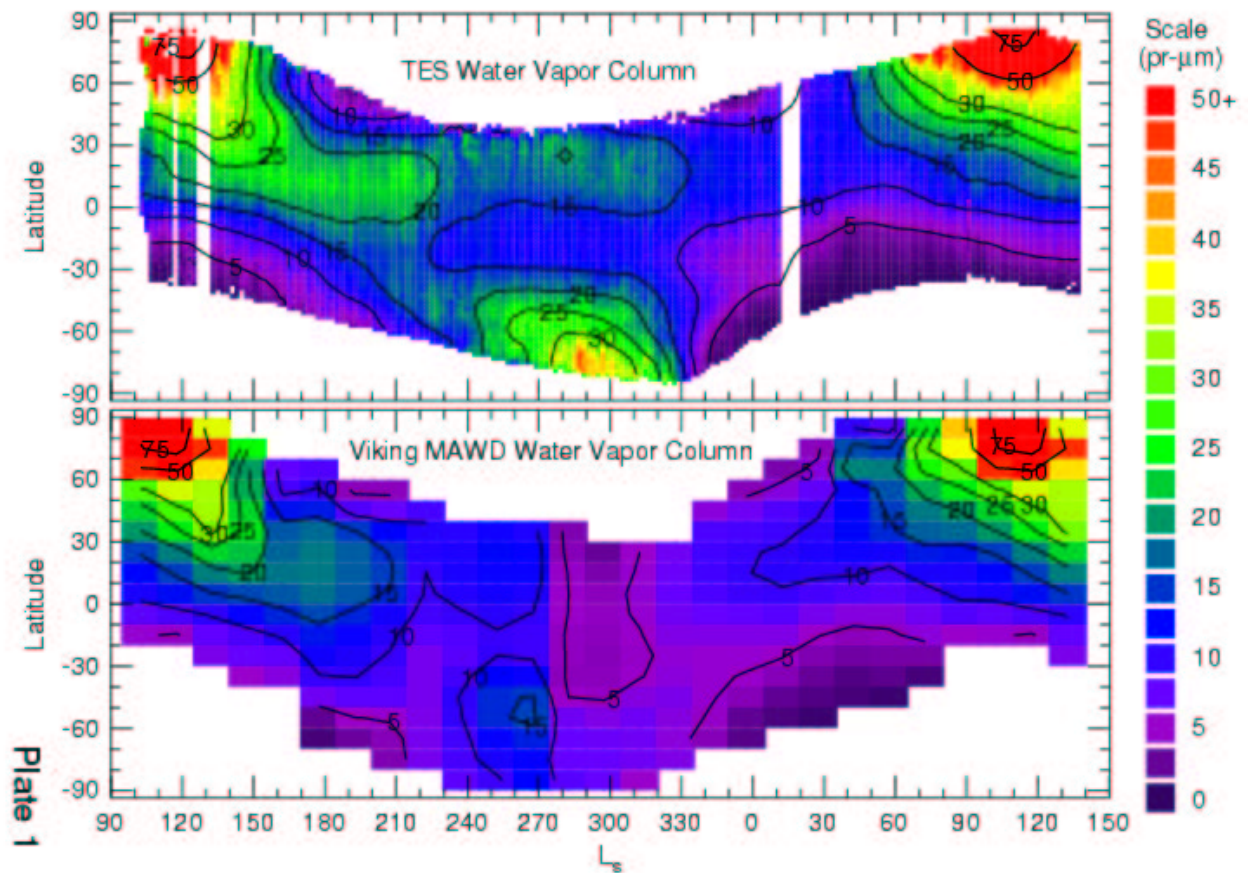


Figure 1.4: One Mars year of MAWD (Jakosky and Farmer, 1982) and TES (Smith, 2002) zonally averaged afternoon observations, as a function of latitude and season : Water vapor column abundance in precipitable microns. Note the great similarity between the two maps, though the MAWD map was obtained twenty years before the TES one, and without detecting any source at the southern summer pole. The areas without data corresponds to the extension of the seasonal caps.

It is vital for us to note that all our assumptions here are still subject to controversy. Our aim is not to enter in this controversy, we will try to be as neutral as possible.

Water in Mars can be present in two phases : solid and vapor. Indeed, the triple point of water is located at (273 K, 6.1 mbar). So, within the Mars surface and atmosphere range of temperature (see above) and pression (always more or less 5 to 10 mbars), there is only a small area where water can be present. Anyway, in our simulations, we will always be in the vapor-solid equilibrium case.

There are several formulas for the saturation water vapor pressure. The model we will use refers (see also [16]) to the formula from Buck (1981), adapted for the typical cold temperatures of Mars :

$$P_{sat}[mbar] = 6.11 \exp\left(21.875 \frac{T - 273.16}{T - 7.66}\right)$$

We give here a few useful definitions. **Humidity** is a measure of the amount of water vapor in the air. One way to represent humidity is the **mixing ratio**, the number of grams of water vapor in each kilogram of air.

Due to the saturation process, there is an upper limit to the amount of water vapor that can be present in a given mass of air. We usually express **saturation mixing ratio** as the number of grams of water vapor that would have to be "mixed with" each kilogram of air to saturate the air. As the formula above shows, a warmer air is capable of holding more water vapor than cooler air is. Note that this does not mean that warmer air has more water vapor in it than cooler air.

The **relative humidity** is a measure of how much water vapor is actually in the air as a percentage of the air's maximum capacity to hold water vapor. The relative humidity is a fraction of mixing ratio on saturation mixing ratio. So, relative humidity could change in two ways. Firstly, if the actual amount of water vapor in the air changes, and secondly if the maximum capacity of the air to hold water vapor changes (so, if the temperature of the air changes).

The point of saturation in water vapor is easily reached in Mars' atmosphere. But, if we compare to the temperature and pressure conditions, we see that the absolute quantity of water is low (only several precipitable microns, $pr - \mu m^2$). Consequently, the thin, cold martian atmosphere can hold little water vapor once saturated. The total amount of atmospheric water on Mars is equivalent to 1 to 2 km^3 of ice. The terrestrial atmosphere holds the equivalent of 13,000 km^3 of ice, but its stratosphere holds an amount comparable to Mars. However, the relative humidity of the stratosphere is much lower than that of the less massive (by a factor of 5) martian atmosphere. Thus, the terrestrial stratosphere is dry, whereas the colder Martian atmosphere is closer to saturation.

Water cycle

One of the aims of the water vapor simulations made (see for example the article of Richardson and Wilson, 2002 [15]) was to reproduce the results given by the observations of the MAWD, and more recently, the TES instruments (see figure 1.4).

The behavior of water vapor in the atmosphere, seen in this figure, strongly reflects the compositionnal asymmetry in the summer caps. When water ice is exposed at the North pole (that is to say, during late northern spring and early summer, when it is illuminated and free of its seasonal CO_2 frost cover), it sublimates into the atmosphere and produces the approx. 100 $pr - \mu m$ maximum that occurs over the North pole. Some of this water is transported equatorward by the atmosphere. In the southern hemisphere during summer, a maximum can also be seen, but it is about a factor of 2 smaller than in the North.

On Earth, the mechanism for carrying out the water vapor transport are the Hadley circulation and wave transport. The Hadley circulation moves water vapor into the equatorial regions in its lower branch. Adiabatic cooling of the moist air in the rising branch removes vapor through precipitation, while the release of latent heat helps drive the upward motion. In the subtropics, the sinking air is

²This unit corresponds to the depth liquid water would have by condensing out all the water vapor in a column of air of unit cross-sectional area ; we have $1 pr - \mu m = 1000 kg.m^{-2}$

warmed by adiabatic compression, reducing the relative, but not the specific, humidity (this produces a cloud-free region). The transport to higher latitudes is accomplished by the correlation of longitudinal variations in the poleward (equatorward) winds with regions of greater (less) water vapor ; this is the so-called "eddy-flux", as it depends upon the character of eddies (i.e. longitudinal variations) in the meteorological fields. The atmospheric transport of Mars is not as fully known as on Earth. We can only make some hypothesis while comparing the Martian circulation, seen above and in [4, 3, 18], and the Earth's, including the difference of origin of atmospheric water on the two planets. Consequently, we assume that, at the solstices, the single Hadley cell may be one process accounting for the transport of water vapor from the North to the South, and *vice versa*.

The minimum observed abundances are less than several $pr - \mu m$ and occur over both polar regions during winter where temperatures reach 150 K. Because their temperature is fixed at the CO_2 frost point (that is to say 148 K), the seasonal CO_2 caps act as a sink for any atmospheric water vapor that is brought in contact with them. During spring, however, as the cap retreat they release water back into the atmosphere. The source for the southern hemisphere maximum may be water released by the retreating south seasonal cap. Alternatively, it may be water that is desorbing directly from the regolith (the unfrosted ground reservoir). However, the regolith can serve both as a source and as sink for water vapor, as water vapor may be also adsorbed as ground temperatures cool in late summer and in fall.

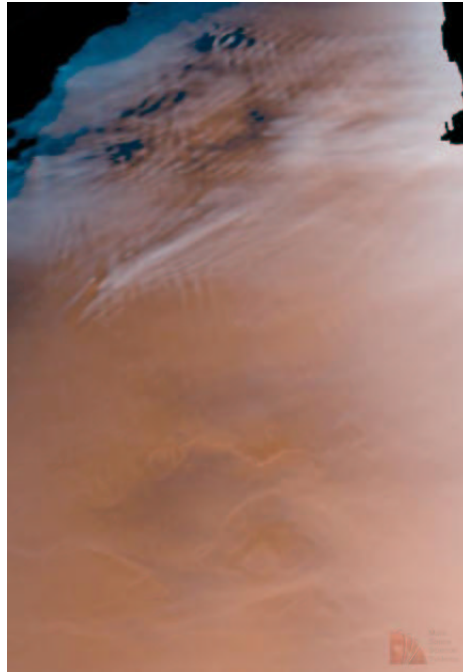


Figure 1.5: Ice clouds and fog (image obtained by Mars Global Surveyor's camera on June 4, 1998)

Water vapor readily condenses in the Martian atmosphere to form clouds (figure 3.1). However, typical cloud water contents are quite low (several $pr - \mu m$). Clouds have been observed to form as low-lying fogs, high-altitude hazes, convective clouds, and clouds associated with fronts and lee waves.

The optically thicker ice clouds occur in two distinct regions : along the edge of the polar caps, and in the tropics during northern summer. The cap edge clouds are associated with what is historically referred to as the "polar hood". They form during winter owing general cooling and during summer owing to the release of water from the retreating cap. The cap edge clouds in the North are more optically thick than those in the South. The northern summer tropical clouds are mostly widespread hazes. These hazes are most prevalent during northern summer because this is the time of year when water vapor abundances are high and tropical atmospheric temperatures are cool.

To put in a nutshell, the water cycle at the current epoch or at other epochs is determined by the behavior of the polar caps and, therefore, by the seasonal CO_2 cycle. Subtle differences in the energy balance at the poles can dramatically change the seasonal behavior of atmospheric water (see [9] for more precision).

There may be direct interactions between the two cycles as well. Condensation of water and CO_2 together may be responsible for depositing the former in the polar region (like Pollack proposed in 1979), although the importance of such a process is uncertain. Also, the condensation wind associated with the CO_2 cycle may be important in the net transport of water vapor (see [15]). Similarly, there are clear interactions between the atmospheric water and airborne dust, and between the water and dust cycles. Dust affects the atmospheric temperature, dramatically influencing the atmospheric holding capacity and the degree of saturation of the water within the atmosphere. Transport of dust and water together may be important, with condensation for water and sedimentation for dust being the only ways to separate the two species, and neither process appearing to act with great efficiency.

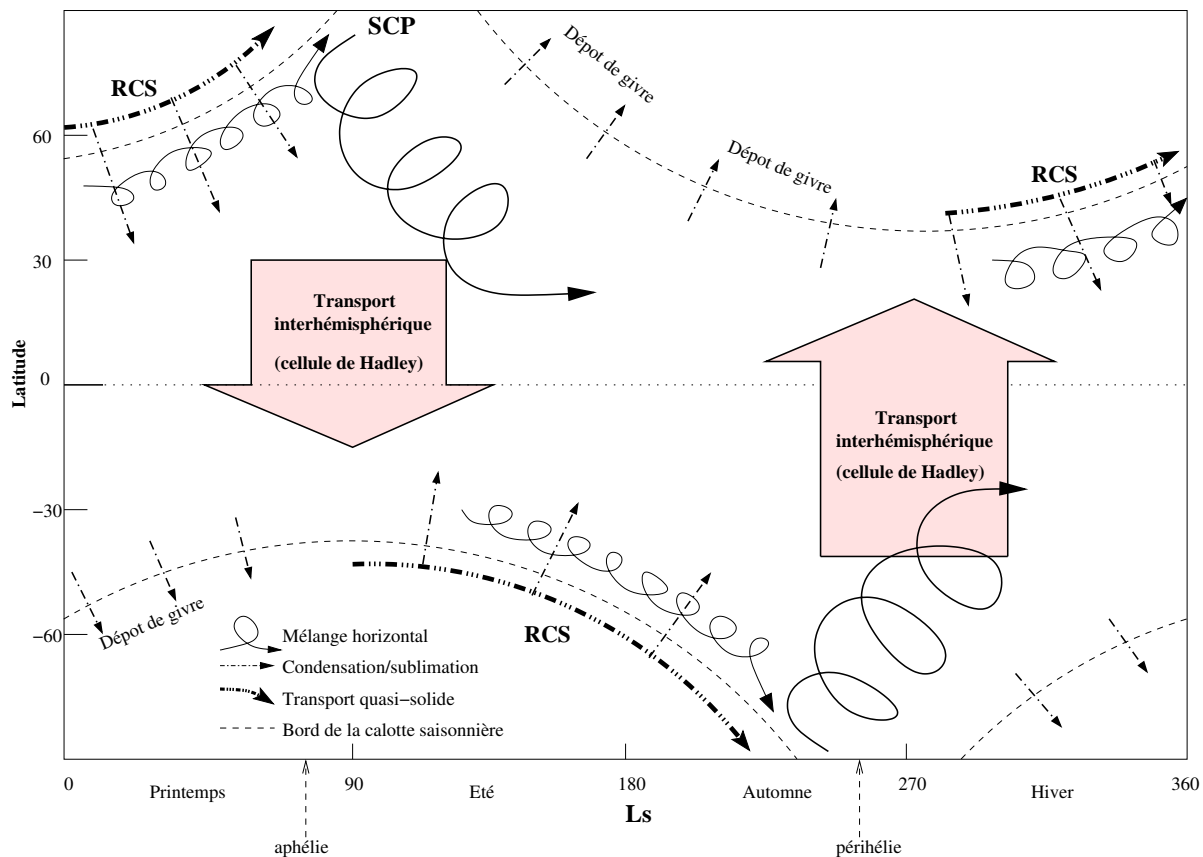


Figure 1.6: Schematic water cycle on Mars [14]. The arrows show the direction of water transport

The figure 1.6 taken from [14] summarizes the annual water cycle on planet Mars. RCS means retreat of the seasonal cap, a process that transport water in a "quasi-solid" way : the water vapor is transported and immediatly re-condensated. Thus, H_2O seems to "follow" the retreating CO_2 seasonal cap. This process leads, for the summer hemisphere, to a seasonal water ice deposit concentrated only on the summer pole (see the northern pole at $Ls = 90^\circ$, and the southern pole at $Ls = 270^\circ$). SCP means the sublimation of the permanent cap. The circle and solid arrow indicate horizontal mixing. It represents a mechanism of diffusion that is responsible for transport of water in the same hemisphere (i.e. not like the Hadley cell inter-hemispheric transport), and account for the relative stabilization of the water cycle on Mars. Of course, the processes are far from being completely known.

Dust

We will not describe precisely the dust cycle (see [2]). We will mention only general facts.

The surface of Mars is mantled with a fine dusty material that is lifted into the atmosphere when surface winds become strong enough to initiate particle motion. Because of the low density of the Martian atmosphere, dust-raising winds must be quite strong. Surface winds gusting to 30 m.s^{-1} were measured by the *Viking 1 Lander* during the passage of a dust storm. Apparently, this is the minimum wind speed required to initiate lifting. However, the dust-raising process is complicated and the threshold for lifting can vary depending on surface properties and atmospheric stability.

Numerous dust storms occur each Martian year and are generally classified according to size. From the smallest to largest, they are dust devils ($< 10^{-1} \text{ km}^2$), local storms (10^3 km^2), regional storms (10^6 km^2), and planet-encircling storms ($> 10^6 \text{ km}^2$). In general, the smaller storms have shorter lifetime and occur much more frequently than the larger storms.

The mechanisms responsible for the Martian dust storms are poorly understood. Dust devils are probably related to strong daytime convective heating as they are on Earth. For the larger storms, however, feedback effects are probably important. The most important feedback is the dust heating feedback. Suspended dust particles warm the atmosphere by direct absorption of sunlight. This then intensifies the circulation, which lifts additional dust. This positive feedback continues until the dust loading is so high that the atmosphere stabilizes and further lifting is suppressed.

1.3 Radiative influence of atmospheric components

1.3.1 CO_2

Except during very dusty periods, and due to CO_2 radiative properties, the atmosphere of Mars is semi-transparent to solar radiation, so there is less heating of the atmosphere by absorption of solar radiation than on Earth. Consequently, its temperature structure is mostly influenced by thermal emission from the surface.

Approximately 10 – 20% of the radiation emitted by the surface is absorbed in the atmosphere. Indeed the CO_2 absorption, negligible for solar radiation (value of about 1%), is important in the thermal infrared, due to a strong absorption-emission band around $15 \mu\text{m}$ [16, 18]. Some of the absorbed radiation is re-radiated back to the surface, producing a modest greenhouse effect. A convenient measure of the greenhouse effect is the difference between the average surface temperature T_s , and the planet's effective temperature T_e . For Mars, this difference is about 5K. By comparison, the Earth's atmosphere produces a much stronger greenhouse effect ($T_s - T_e$ approx 35K) - but the main radiative component is water vapor, and not CO_2 .

1.3.2 Dust

The radiative effect of dust is stronger than CO_2 . The temperature profile is increased of about 10K, due to solar radiation absorption. Based on *Pathfinder* measurements, the mean particle radius is approximately $1.7 \mu\text{m}$. Particles in this size range interact efficiently with sunlight and less so with thermal radiation. During the *Viking* mission, the daily mean temperature at the *Viking Lander 1* site declined by several degrees kelvin during the passage of a dust storm. This suggests that dust particules produce a modest greenhouse, and reflect more sunlight back to space than they emit to the surface.

1.3.3 H_2O and other radiative components

Unlike Earth, ozone on Mars is not generally present in concentrations great enough to contribute significantly to atmospheric radiation, except perhaps at the edge of the polar night.

Water vapor is also present in amounts too small to affect significantly atmospheric heating and cooling either through its direct radiative effects at infrared wavelengths or through latent heating. We will, of course, see that the radiative effect of water vapor is no more negligible at high obliquity, where the water cycle releases important amounts of water vapor in the atmosphere. Precisions will come later - it is one of the main topic of this report (see [16] as an introduction).

The formation of ice clouds (figure 3.1) can affect radiative heating of the atmosphere and of the surface, and this provides a mechanism for atmospheric water to affect the circulation. The clouds themselves further reduce atmospheric temperatures. Atmospheric heating, occurring when sunlight is absorbed by the dust, is reduced when ice forms around the dust particles and causes dust to gravitationally settle to the ground.

However, because of the spatial coverage of ice clouds, except for the polar hoods, the IR effect is quite limited in space and time, it has been generally assumed that their effect on large-scale motions is not significant. Optically thick ice clouds are most extensive and persistent in the polar night above the seasonal polar cap. These polar hood clouds might affect the polar radiative balance by increasing the downward infrared flux to the surface and thus reducing the rate of condensation of CO_2 . By scavenging suspended dust from the atmosphere, ice-cloud formation can affect atmospheric cooling in the polar night, while the scavenged dust may alter the surface visible albedo and thus the rate of CO_2 sublimation when sunlight returns to these regions at the end of the winter.

Chapter 2

Background and preliminary analysis of the high-obliquity Mars paleo-climate

2.1 Basic facts about paleo-climates

2.1.1 Climate changes throughout ages

It is now quite certain that Mars have experienced significant climate change. Today, Mars is cold and dry, yet spacecraft images provide striking evidence that the planet's climate was different in the past. Layered terrains in the polar regions may have been created by climate change associated with astronomical variations on Mars' orbital parameters. Valley networks and degraded craters in ancient terrains may be the result of a thicker atmosphere early in Mars history. And there is some evidence that the planet may have had an ocean at some time in its past, perhaps on several occasions. Thus, Mars is an ideal laboratory for comparative meteorological studies and it may provide insights into the mechanisms responsible for climate change here on Earth.

We can basically consider three distinct climate regimes :

1. Very early in the planet's history (> 3.5 Ga) when warm and wet conditions are thought to have prevailed, because of some greenhouse effect compensating a "faint young sun".
2. The planet's middle history (3.5 - 1 Ga) during which episodic ocean formation has been suggested. During this period, Mars seemed to lose a great part of its atmosphere - as a result, the climate should have grown colder.
3. Recent areas in the planet's history (< 1 Ga) when orbitally-induced quasi-periodic climate change is thought to have occurred. This changes took great importance when trying to explain the present-day Mars geology.

We will now particularly look at the last period we've described. The main clue that geologists use are the polar layered deposits (see figure 2.1). Both polar regions on Mars are characterized by extensive layered terrains, which are among the youngest geological features on the planet. The layered structure consists of series of plates of varying thickness that are stacked one upon the other. The fact that they are continuous and uniform suggests they were formed by atmospheric sedimentation processes that were modulated in time. The leading theory on the origin of the layered terrains is the astronomical theory [11], which predicts variations of Mars' orbit parameters.

2.1.2 Obliquity variations

The Mars' orbit parameters undergo significant variations. Indeed, Mars lacks a large moon, and is strongly perturbed by relatively nearby Jupiter - consequently its obliquity and eccentricity vary much more than do those for the Earth. As seen on figure 1.1, the present obliquity is 25.2° . However, during the past 5 millions years, its obliquity has varied between 15° and 45° , and its eccentricity

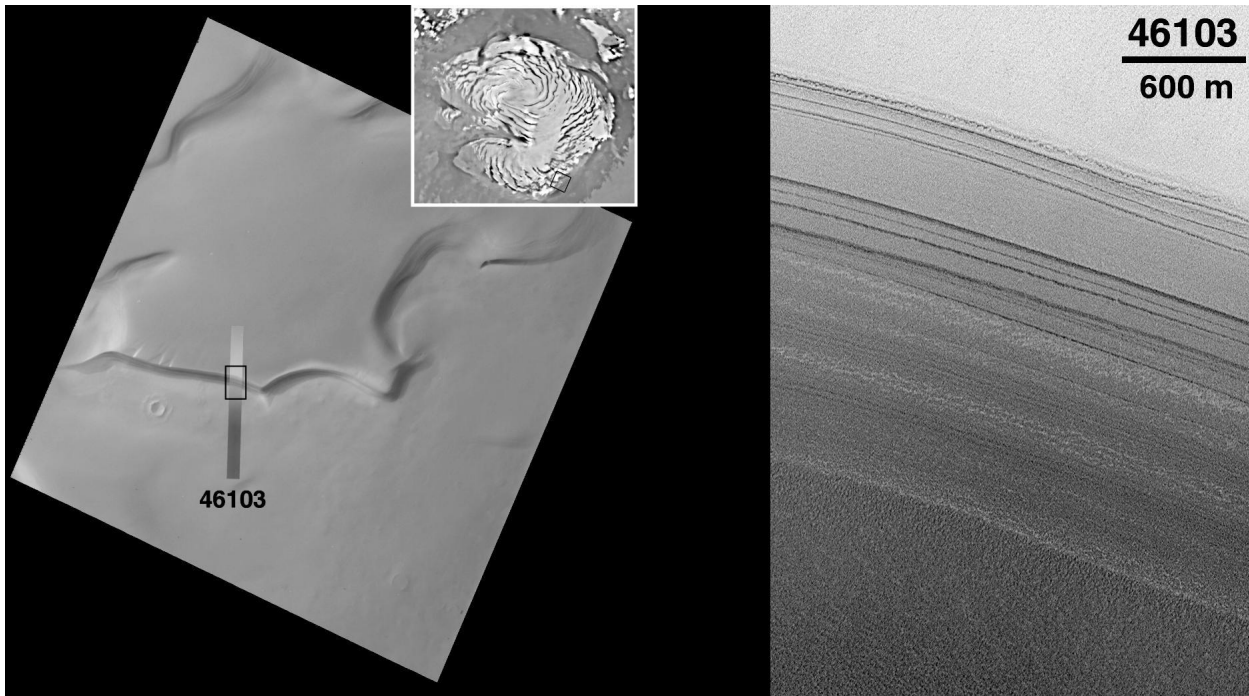


Figure 2.1: Layers on the North Polar Cap. The martian North and South polar regions are covered by large areas of layered deposits. Since their discovery in 1978 (Viking Orbiters), these polar layered deposits have been cited as the best evidence that the martian climate experiences cyclic changes over time. It was proposed that detailed investigation of the polar layers (e.g., by landers and/or human beings) would reveal a climate record of Mars in much the same way that ice cores from Antarctica are used to study past climates on Earth. The polar layered deposits are thought to consist of 10 to 100 layers each between 10 and 100 meters (33 to 330 feet) thick. The layers were proposed to have formed by slow accumulation of dust and ice - perhaps only 100 micrometers (0.004 inches) per year. A layer 10 meters (33 feet) thick would take 100,000 years to accumulate, roughly equal to the timescale of climate changes predicted by computer models. The image shown here was taken on July 30, 1998, near the start of the 461st orbit of Mars Global Surveyor. The picture shows a slope along the edge of the permanent north polar cap of Mars that has dozens of layers exposed in it. The image shows many more layers than were visible to the Viking Orbiters. The layers appear to have different thicknesses (some thinner than 10 meters (33 feet)) and different physical expressions. Some of the layers form steeper slopes than others, suggesting that they are more resistant to erosion. The more resistant layers might indicate that a cement (possibly ice) is present, making those layers stronger. All of the layers appear to have a rough texture that might be the result of erosion and/or redistribution of sediment and polar ice on the slope surface

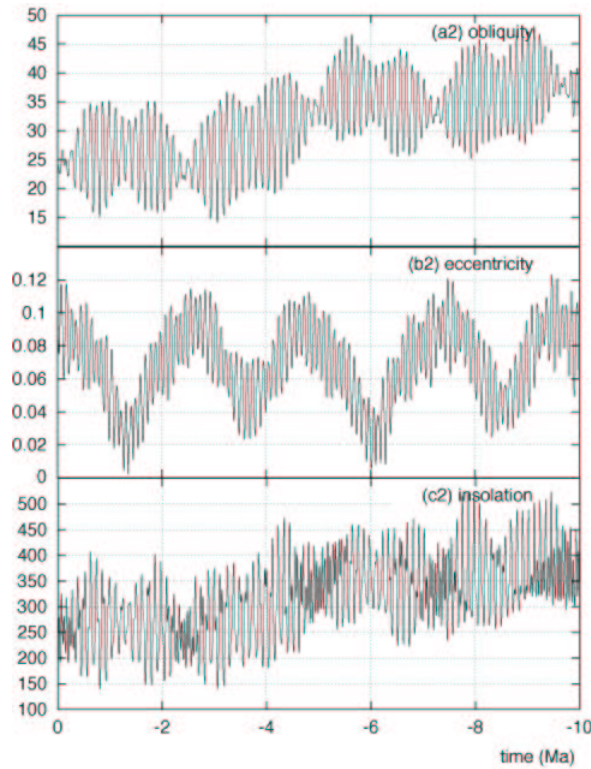


Figure 2.2: History of Mars' orbital parameters changes - and its consequence on insolation [11]

has varied between 0 and 0.12 (see figure 2.2). Both these parameters have a primary oscillation frequency of approx. 10^5 year that is modulated on a 10^6 year time scale. The spin axis (season of perihelion) precesses with about a 50,000-year period. Beyond 5 myr or thereabouts, orbit calculations [11] suggest Mars is in a large chaotic region with obliquities ranging from 0° and 60° .

Of the three main orbit parameters, obliquity exerts the strongest influence on the climate system. Changes in obliquity alter the latitudinal variation of solar insolation (see figure 2.3). The poles receive an increasing amount of insolation as the obliquity increases, while equatorial insolation decreases. Above 54° obliquity, the poles receive more annual average insolation than the equator. Such changes in the pattern of insolation can have a profound effect on ground temperature, on the distribution of volatiles around the planet, on the general circulation, and on the frequency and location of dust storms [17] (see figure 2.4).

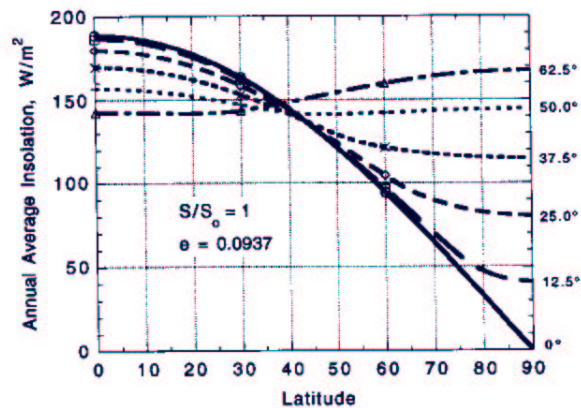


Figure 2.3: Effect of obliquity changes on insolation

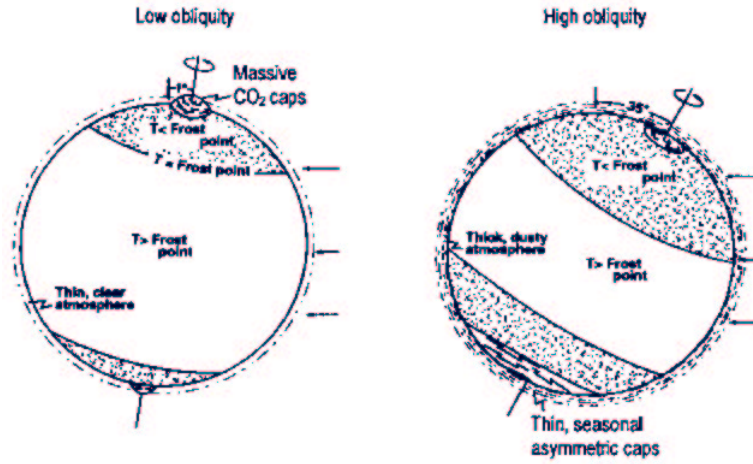


Figure 2.4: Quasi-periodic climate changes : a summary [10]

2.2 The Ames Mars General Circulation model

2.2.1 Introduction to the model

We use the Ames Mars General Circulation Model (GCM), a climate model that has given a lot of interesting results, including a rich description of the Mars general circulation [4], validated later by another model from Forget et al. article [3]. Furthermore, some MGCM simulations have been used to interpret selected results from the Mars Pathfinder atmospheric structure instrument/meteorology experiment [5].

Ames GCM includes 3-D dynamical code ¹, coupled with physical modelisations :

- radiative transfer
- convection
- condensation / sublimation of CO_2 and H_2O
- sedimentation - lifting of dust
- sub-grid scale topography effects
- soil thermal model

Given a initial state of T, P, wind fields, and fundamental physics and fluid mechanics laws, the program computes the future evolution. We must mention that the "dynamical" part and the "physical" part are very different : for example, they do not share the same integration scheme. Actually, as the dynamical code calculate exchange between vertical columns (making 3D calculations), the physical code calculate 1D tendencies, within each columns, with the conditions given by the dynamical variables (pressure, temperature, wind fields, tracers) (see figure 2.5). The physical part is not called each timestep of the dynamical calculation, for reasons of numerical stability and usable CPU time.

The MGCM is continuously undergoing updates and improvements. The GCM 2.0 was still a work in progress when we started some high-obliquity simulations. However, the major updates planned have been made : the new GCM features an improved C-grid dynamical core, a new radiation code, based on a generalized 2-stream model, and a efficient tracer transport scheme for an arbitrary number

¹based on the planetary version of the fluid mechanics equations [12]

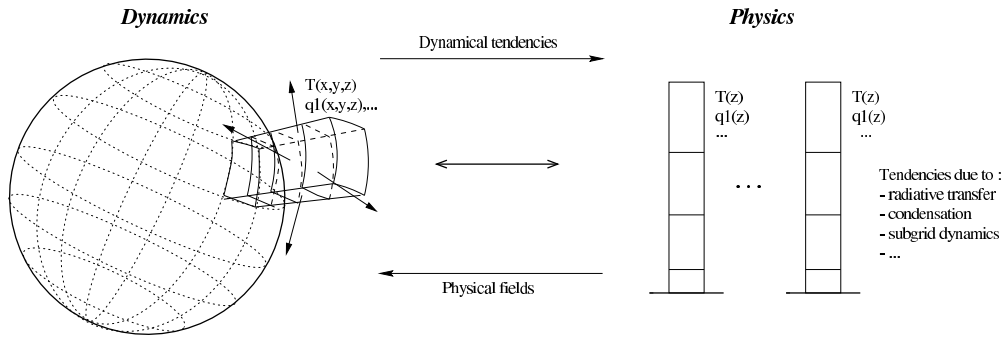


Figure 2.5: Interaction between the two main parts of a GCM

of tracers. The model includes the radiative effect of CO_2 , H_2O , and dust, and runs with recent MOLA topography, consortium albedo and thermal inertia.

The Ames GCM is also featuring a sophisticated model for cloud microphysics, brought by Montmessin [14]. This model features highly precise modelisation of clouds formation processes (nucleation, condensation/sublimation, sedimentation/accretion). Unfortunately, the inclusion in the model of radiatively active water ice clouds was still difficult, for numerical reasons.

2.2.2 Simulations done

These breakthroughs allow us to launch simulations of Mars' climate and volatile cycles at an improved degree of precision. All the high-obliquity simulations done before ² did not include the water vapor radiative effect, neither such high-precisely simulated clouds formation in a 3D simulation. What lacks the model is mainly the radiative role of water ice clouds, but this problem may be solved in few months, and the work we started with Haberle's team may lead to a publication at the end of the year.

The model we use has no pretention to be fully realistic. The aim is to focus on some aspects of high-obliquity Mars, mostly about the water destination, could it be vapor, clouds, or ground ice. For dust, we specify fixed optical depth uniform in space and time at the 6.1 mbar reference level. However, dust is an active tracer, so as the model can efficiently simulate the nucleation of water ice, and the atmospheric transport of dust. Another simplification is to keep the value (and the behavior) of pressure like present day Mars ³. Of course, as the obliquity changes, the distribution of volatiles around the planet is modified, and it has consequences on the pressure. However, our simulations do not include this type of correction. In addition, let us mention that we work, for reason of time, at low resolution: the latitude - longitude grid was 24x16 (a grid box is Lat 7.5° x Lon 22.5°), and we use 24 vertical layers. 40 points of longitude may give more precise results.

The model features a complete CO_2 cycle, including the seasonal behavior of the polar caps, mainly on the South, were the CO_2 cap is thicker than in the North. We add to the model a Permanent water ice cap in the North Pole, like it is observed for present Mars, and likely to be also present at the past obliquity cycles. The model do not simulate any regolith - it is basically a climatic model.

The philosophy of our simulations is simple : take present Mars, turn obliquity, and analyze the results we obtain. Corrections should be included, as we do some simplifications. However, our simulations are a good basis for supporting the attractive hypothesis of natural changes brought by obliquity cycles.

We choose to launch some simulations for obliquity 35, 45, and mostly 60° obliquity. The table 2.6 summarizes the simulations launched. We have done 7 complete Mars years of simulation. 7 years is enough to have significant results for the 60° case (the water cycle takes three years to reach equilibrium). However, for others obliquities, the water cycle takes more than seven years to reach

²see [15, 7] and the recently published Mischna et al article [13]

³surface pressure of 6.1 mbar

equilibrium, even if the results are usable to analyze the situation at these obliquities. We write outputs every 72 hours (consequently we do not see the diurnal cycle).

Simulation	Obliquity	H_2O vapor radiative effect	τ_{dust}
[noH]	60	no	0.3
[H]	60	yes	0.3
[o35]	35	no	0.3
[o45]	45	no	0.3

Figure 2.6: Simulations launched

2.3 Quasi-periodic climate changes : an overview with a preliminary analysis of simulations

2.3.1 Ground temperature

As the obliquity increases, the polar regions warm with respect to the equator, as shown in figure 2.7 (compare to Haberle et al. [7]). Higher obliquity situation leads to higher summer pole ground temperature, and consequently higher contrast between pole and equator. At 60° obliquity, in the southern summer ($L_s = 270^\circ$), ground temperature reaches nearly 310 K, while the 30° obliquity value is no more than 280 K. The behavior of the polar caps follows the ground temperature tendencies. When the obliquity is higher, the seasonal polar caps extends to the equator - as a result the gradient of ground temperature from the equator to the pole grows.

2.3.2 Volatile cycles

The ground temperature is a key parameter for the CO_2 and H_2O cycles, as seen in the chapter 1. Its behavior as the obliquity increases has two important consequences. First, any CO_2 stored in the high-latitude regolith will be driven into the atmosphere, thereby increasing surface pressures (15 mbar at 55° obliquity). Higher surface pressures lead to greater dust lifting and greater dust transport into the polar regions⁴. Second, water ice will be driven off the pole and into low-latitude reservoirs such as permafrost. Thus, polar layers forming at high obliquities would be dominated by dust.

Jakovsky and Carr [8] first suggested that during periods of high obliquity, polar surface ice would be sublimated and transported away from the summer hemisphere polar cap and to the equatorial region, where it would be deposited, forming a perennial ice "belt". Indeed, the water content of the nonpolar atmosphere may exceed the saturation holding capacity, and water-ice deposits may become more stable in the equatorial and mid-latitudes than at the pole. The rate at which such a belt would be formed depends on the flux of water vapor from each polar cap during its respective summer, which itself depends on the vapor gradient from pole to equator, and such dynamical considerations as wind speed and turbulent mixing.

We have seen in the previous chapter that the quantity of water vapor in a column hardly reaches $100 \text{ } \mu\text{m}$ (figure 1.4) in the summer pole. On annual average, we get between 10 and $20 \text{ } \mu\text{m}$ of atmospheric water vapor. The atmosphere remains saturated only in the high latitudes, and in the tropics, it falls well below the saturation vapor pressure, and so surface ice is unstable. As obliquity is increased, however, cap temperatures rise, placing considerably more water vapor into the atmosphere - up to $3000 \text{ } \mu\text{m}$ at 60° obliquity (see figure 2.8). Our results are close to the results of Richardson and Wilson [15], performed with another GCM. The atmosphere is extremely wet, as expected with Jakovsky and Carr suggestions. Peak water amounts in both hemispheres occur in the polar regions on

⁴Haberle et al. [7] showed that this greater dust lifting was a result of an enhancement of the solstices general circulation, including low-level "monsoon" jet associated with a well-developed cross-equatorial Hadley circulation.

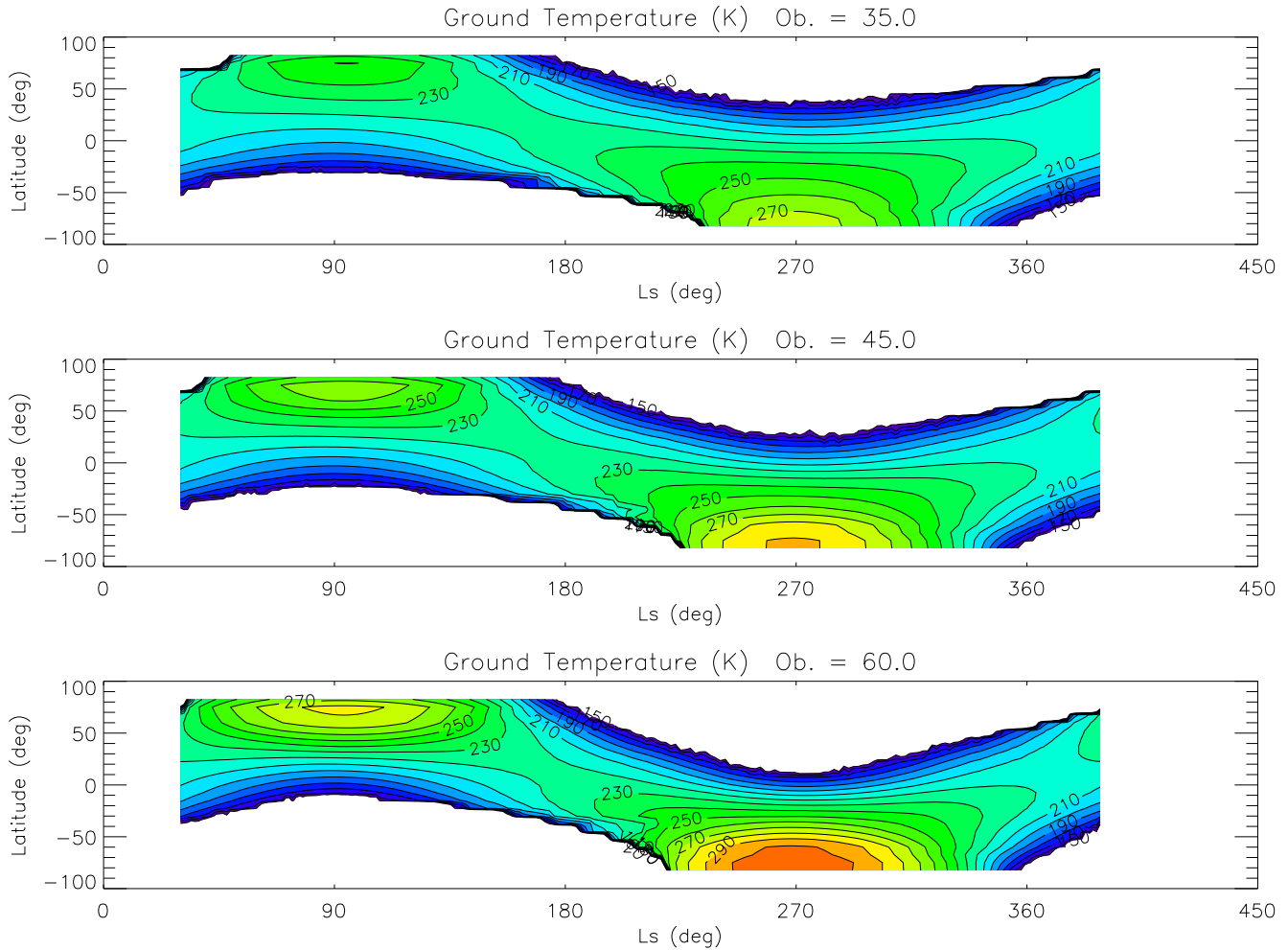


Figure 2.7: Ground temperature, for three different values of obliquity (simulations [o35],[o45] and [noH]), as a function of latitude and season. The asymmetry between the Northern and the Southern hemisphere is due to the eccentricity of the planet, which is near 0. The blank areas represent the extension of the seasonal ice caps, where ground temperature is given by the CO_2 frost point (around 150 K)

their respective summer - as expected, when glancing at figure 2.7. The mechanism described in figure 1.6 is still valid at high obliquity, and seems to be greatly enhanced. We should note that the peak water amounts in the southern hemisphere are much shorter lived and more latitudinally constrained than in the North. We should also mention that some significant amounts of dust in the polar deposit can lower the quantity of water ice sublimated in the atmosphere. It is very interesting that our model includes water vapor as a radiatively active component. We have seen that present day Mars undergo no significant radiative heating or cooling by water vapor, for the amounts are negligible. Such a huge release of water vapor at high obliquity will logically lead us to study its radiative effects (see chapter 4).

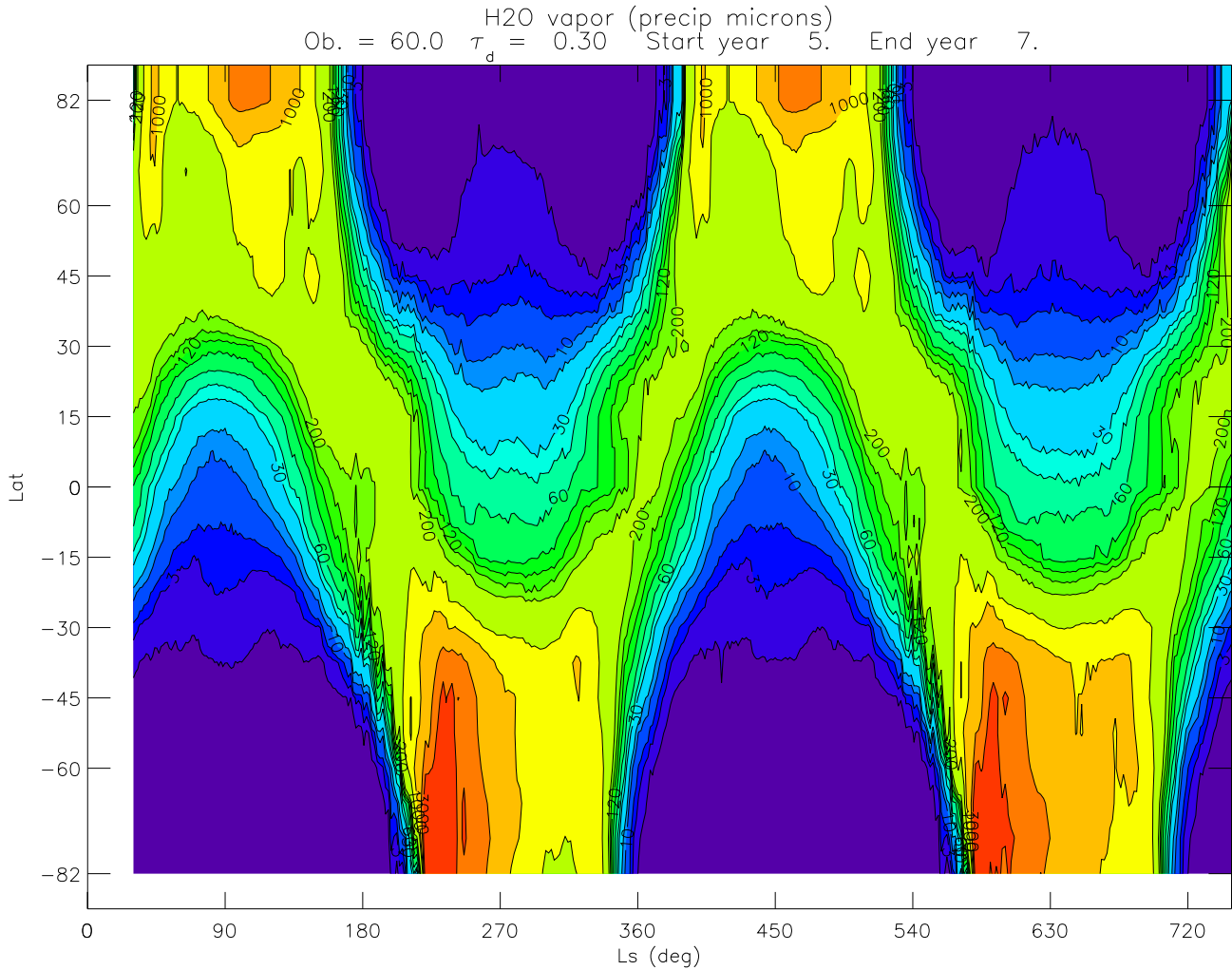


Figure 2.8: Obliquity 60, simulation [noH], water vapor column abundance in precipitable microns : zonally averaged, function of latitude and season

At low obliquities the opposite occurs. The polar regions cool with respect to the equator. CO_2 migrates back into the high-latitude regolith and eventually the atmosphere freezes out, forming permanent CO_2 ice caps. The surface pressure fall so low that dust lifting ceases and there is no transport of dust into the polar regions. At the same time, water diffuses out of the low-latitude permafrost and is cold-trapped out at the poles, leading to the creation of an ice sheet whose thickness is limited by the amount of water stored as permafrost and its ability to diffuse through the soil and into the atmosphere. Thus, polar layers forming at low obliquity would be predominately water ice.

This kind of simple mechanism seems reasonably able to account for the polar layered deposit. The black and white layers alternance corresponds to the low/high obliquity oscillation. However, the

theory of quasi-periodic climate change is not definitive. It needs to be precised, as other processes must be involved, but it seems also to be a solid basis for present and future collaboration between the geologists and the climatologists.

Chapter 3

Water cycle in high-obliquity Mars

In the previous chapter, we simply give an overview of the water cycle, discussing mainly about the water vapor behavior. In this chapter, we will bring additional elements, including clouds formation, ice formation and general circulation.

3.1 Main simulation : 60° obliquity case

This simulation was the main simulation we planned to do. Mars rarely reached 60° obliquity, but when it did, it surely underwent dramatic consequences. We called this simulation [noH] previously. In the next chapter, we will see the simulation done when adding the H_2O radiative effect, called [H].

3.1.1 Water vapor

We have seen previously some elements of this subject. Let us just here emphasize the fact that the amounts of water vapor in the atmosphere at high obliquity are huge. TES data (figure 1.4) shows an annually averaged quantity of water vapor of 20 $pr - \mu m$ in the higher latitudes. Our simulation [noH] shows an annual mean of nearly 600 $pr - \mu m$ in the higher latitudes, so we have 30 times more water vapor released in the atmosphere.

The atmospheric capacity of water vapor is constrained by the saturation mixing ratio, which depends on the temperature. Not only more water vapor is released in the atmosphere because the ground temperature is higher at high obliquity : the atmospheric temperature is also higher of about 20-30 K in the summer hemisphere¹, which means that the maximum holding capacity of water vapor in the atmosphere is increasing.

More water vapor is found in the South than in the North, because the South cap is a better trap for water (the CO_2 ice is thicker than in the North), and of course because the Southern hemisphere is warmer during summer than in the North.

All this water vapor condenses in ground ice or ice clouds, what we are going to study now. But we will not consider as surprising the fact that the peaks of clouds formation and ground ice deposits are in the summers.

3.1.2 Ice clouds

As the figure 3.1 shows, the ice clouds seem to mainly form at the tropics. At the equator, however, we see a minimum annual quantity of clouds of 10 $pr - \mu m$. We observe a maximum of 1000 $pr - \mu m$ at the southern summer, in the south tropic. This is a result of the ground ice deposit sublimation. It causes cloud formation, because water vapor is released in the atmosphere, but the temperature is low enough to allow some clouds to form, as water ice nucleates on dust.

The clouds are low and thick clouds. At normal obliquity, the radius of ice clouds particles never reaches more than 5 μm . Here, radius increases to the value of 30-50 μm in the southern summer,

¹compare 4.2 in next chapter and for example figure 8, article [3]

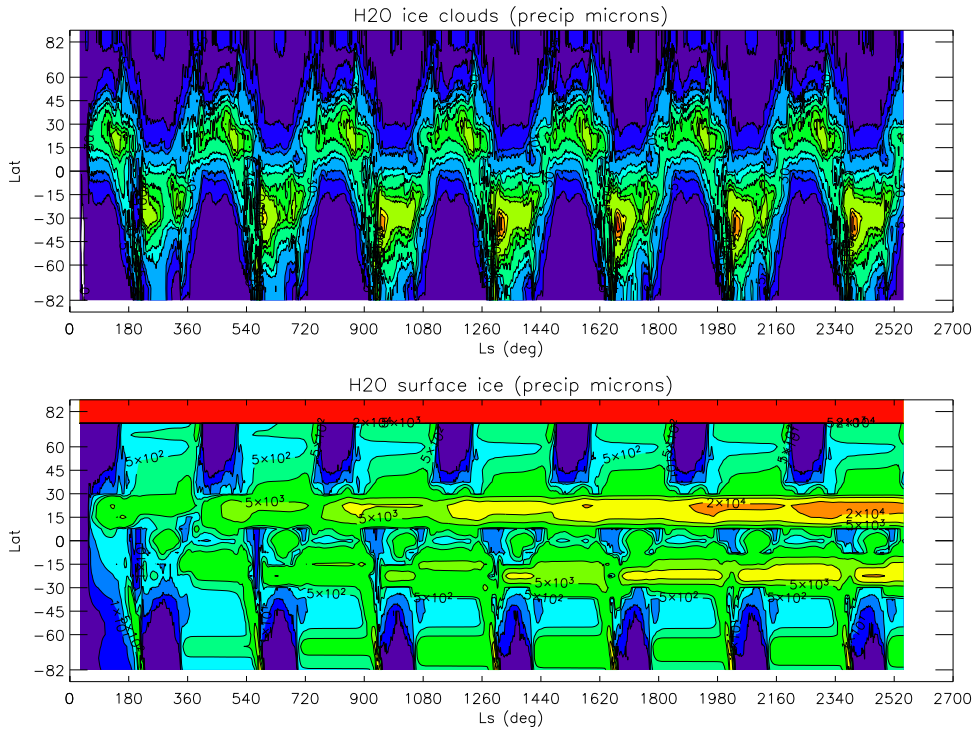


Figure 3.1: Water ice clouds and ground water ice, simulation [noH], zonally averaged, function of latitude and season. The levels are 0 1 5 10 30 50 100 150 200 500 700 1,000 in $pr - \mu m$, for the clouds and 0 1 10 100 500 1,000 5,000 10,000 20,000 in $pr - \mu m$, for the ground ice

and 15-30 μm in the northern summer. The opacity of such a seasonal cloud belt is $\tau = 30$ in the first case, and $\tau = 12$ in the second case.

This last assumption tends to show our model really lacks a cloud radiative effect scheme - this is presently a work in progress.

The bigger particles of clouds in the high-obliquity case fall out faster than those for present obliquity. It is surely one factor that could explain that more ice is found on the ground, Let us analyze more precisely now the ice deposit on the ground.

3.1.3 Ground ice

We are still analyzing the same figure than previous subsection, but we concentrate on the bottom plot. We still plotted the seven years of [noH] simulation.

As the obliquity is higher, we observe more water ice falling on the ground than the normal obliquity case, which is *a priori* normal, as more water vapor is released from the Northern polar cap.

The two yellow zones show ice deposits that tend to be stable as year passes. These latitude [15,30] and [-30,-15] zones are predominant destinations for water ground ice, and seems only to slightly undergo the seasonal variations due to the polar cap retreat, in opposition with what happens in higher latitudes, where annual minimum ice is zero. In the equator, the ice deposit is only a little more stable than in high latitudes. Our plot really emphasizes the main deposition on the tropics. The northern deposit reaches 20,000 $pr - \mu m$ (20 centimeters !), as the southern deposit is thinner, "only" 10,000 $pr - \mu m$. This asymmetry is due to the eccentricity, which gives Mars southern summers warmer than northern summers. The asymmetry on the ground temperature causes an asymmetry of the ice deposits. The northern places for ice deposit are more seasonally stable than southern places. In the south, a warmer ground causes a more active sublimation of deposits. We see peaks of clouds formation in latitudes just below the ice deposition, showing that in the south, water reservoirs can more easily than in the North fill or empty.

We chose to make a representation of ground ice with quantities of mass. We integrate the $pr - \mu m$ quantities, all over the planet, taking into account the grid boxes surfaces. For N latitudinal grid points, the mass of water ice ground all over Mars is

$$\sum_{i=1}^N w^i Q_{H_2O}^i$$

$Q_{H_2O}^i$ is the zonally averaged quantity of ground water ice, in $kg.m^{-2}$, obtained with multiplication by 1000 of the $pr - \mu m$ quantities. w^i is the surface, corresponding to $Q_{H_2O}^i$, of a belt drawn between latitude $i-1$ and latitude i :

$$w^i = 2\pi \left| \int_{\lambda_{i-1}}^{\lambda_i} r^2 \cos \lambda d\lambda \right| = 2\pi r^2 |\sin \lambda_{i-1} - \sin \lambda_i|$$

Here is the plot (3.2) we obtain : the quantities are in GigaTons, i.e. 10^{12} kg.

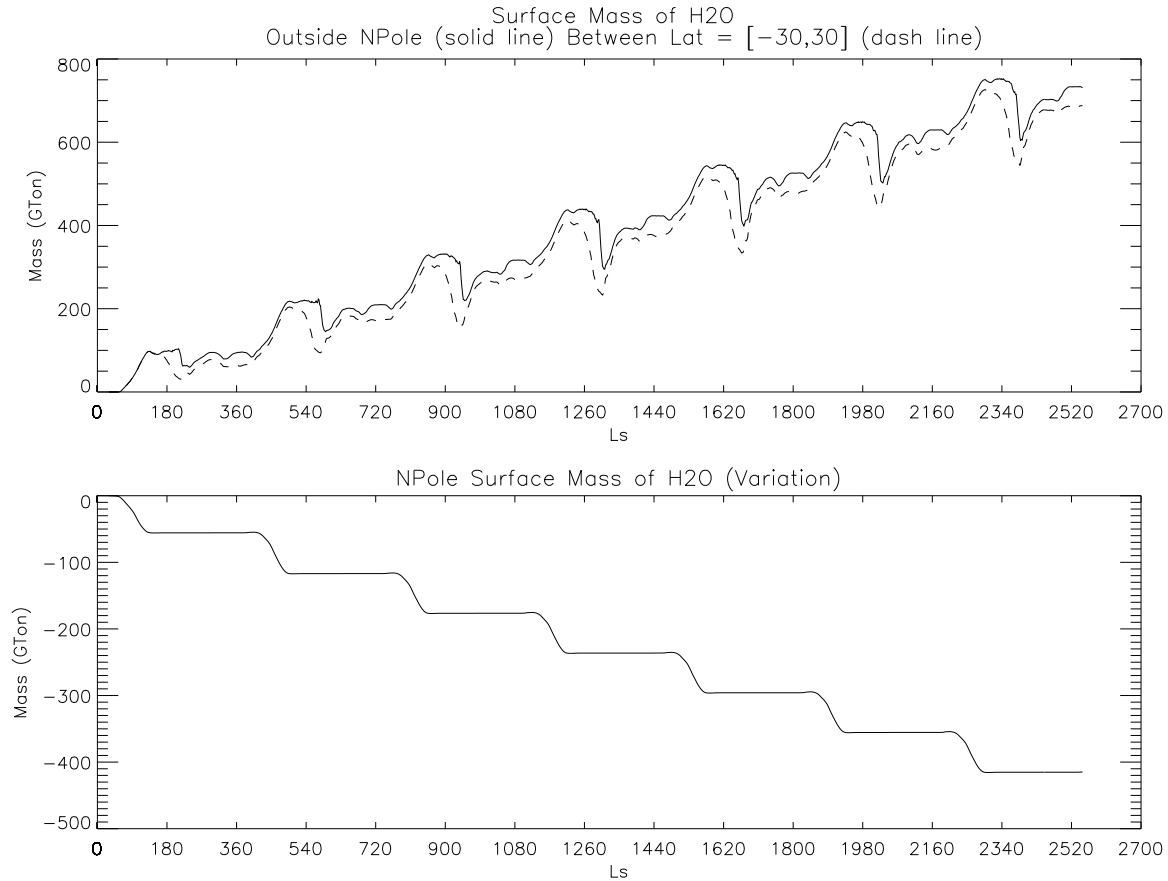


Figure 3.2: Mass budget of water ice ground, as function of season

The top plot shows the ice deposit in every Mars latitude, except the North pole. We easily note that ground deposit is increasing regularly each year. This plot is an indication of the main fact that the water ground ice at the tropics did not return to his source, the North Pole. The bottom plot shows a net loss for the North pole : the water taken is used to increase the water vapor in the atmosphere, to form cloud and ice deposit - but this ice deposit never occur again at the pole, because turning the obliquity to 60 have promoted tropics to be more stable for ice deposition than the poles. The dash line in the top plot shows that the ground ice deposits are concentrated between $[-30,30]$ latitude, something we have seen previously.

It is interesting to calculate how long will the northern polar cap last. It is generally admitted that the northern water cap of Mars can be calculated assuming a layer of 10 precipitable meters of

ice all over the planet. The northern polar cap deposit is consequently $1.32 * 10^6 Gton$. With the loss rate calculated on the bottom plot, we find that it will take 44,000 Earth years to completely exhaust the Northern cap, if we keep the conditions of the simulation [noH]. Even if this result is an approximation, it seems to be an order of magnitude less than the time scale of obliquity changes (10^5 years). That seems to show that a complete disparition of the Northern polar cap may have occurred, if the planet remained long enough in a 60° position.

We will now study precisely the stable places in the planet for ground ice. In the previous plot (3.1), we have seen two stable latitudes for ground ice. We will now get rid of the zonnally averaged quantities, and have a latitude/longitude plot (3.3, including the topography (compare to plot 1.2), and showing in the sixth year the minimum of water ice in the ground. Every dark blue zone has a minimum of zero $pr - \mu m$ all over the year, which means that ground ice is not annually stable in these locations.

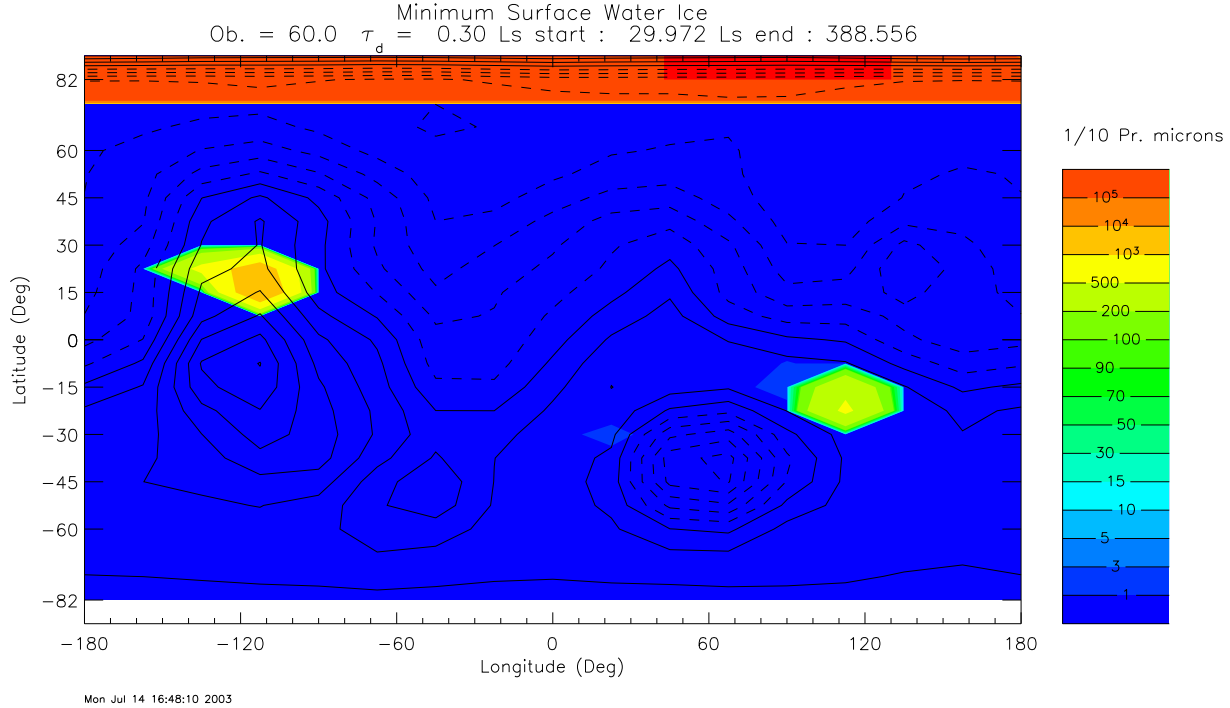


Figure 3.3: Latitude/longitude plot, simulation [noH]. Annual minimum of water ice ground, in precipitable microns. Dark blue means zero.

Even if our spatial resolution is not optimal, our results are similar to Levrard's ², who used the LMD GCM with a higher longitude resolution, and a higher number of years simulated. We found two main places of annually stable ice deposit :

1. Tharsis volcanos, where the minimum quantity reaches more than 100 $pr - \mu m$. The diurnal amplitude of variation for ground ice is about 10 $pr - \mu m$, so Tharsis volcanoes undergo permanent (and quite thick, remember 100 $pr - \mu m$ is a minimum) ice deposit. Olympus Mons seems to be a less predominant place of ice deposit (10-20 $pr - \mu m$). These places are all among the highest mountains on Mars.
2. North-East of Hellas crater (Terra Tyrrhena, Terra Promothei), where the minimum quantity reaches nearly 50 $pr - \mu m$. Here also we conclude there is thick permanent water ice all year long. It is another effect of the topography forcing, because this zone is delimited by the deep Tharsis crater in the South-West, and by a strong decreasing gradient of topography in the

²personal communication by Forget, from Levrard's thesis

North-East. This zone can consequently be seen as a high-topography place, where the winds force the ice to deposit.

Deposits not necessarily form in places where the mean annual temperature is low. The main parameter is the relative humidity, and it depends on the saturation rate. What is consequently important is the thermal structure of the atmosphere, and of course the transport by the atmospheric circulation.

We would like to emphasize that, even if they lack important parameters, the simulations made are hopeful. Our work, made with atmospheric science and physics parametrization, meets with a quite good approximation the geologists' work ³. Some glaciers are thought to have been present on Tharsis and near Hellas, in times when the obliquity changes are also thought to have occurred. The work we started is only the beginning of a closer collaboration between the geologists and the climatologists, and is likely to lead to some interdisciplinary publications.

3.1.4 General circulation

We have seen previously what is the general circulation in the normal obliquity case. For example, around $L_s = 90^\circ$, a single cross-equatorial Hadley cell develops. Typically⁴, the maximum intensity of the mass stream function (averaged between $L_s = 90^\circ$ and 120°) is about $3.10^9 kg.s^{-1}$. Our simulation [noH] gives, for the same value, in the same conditions⁵, $7.10^9 kg.s^{-1}$. On the opposite, the difference at the equinoxes are not so significant, but this is not a real surprise : turning the obliquity of the planet affects much more the solstices than the equinoxes. At the solstices, the axis of obliquity "points" at the sun.

When the obliquity is 60° , the general circulation is not modified, but enhanced. This is not a big change, but it has dramatic consequences. The general circulation is the main agent of transport for volatile components like water vapor, or like aerosols like dust or ice clouds. Let us emphasize that our simulations are done with a Northern permanent polar cap, and that our results show a well-developped water cycle all over the planet. We can wonder how is it possible. We must not forget that it is mainly the general circulation that lead the mechanism of water vapor transport to the southern hemisphere. In this hemisphere, there is no initial source of water vapor : any water comes from the water transported from the North and that have been trapped by the seasonal CO_2 cap during south winter.

3.1.5 Conclusion for Mars at 60° obliquity

In comparison with the present obliquity case :

- ground and atmospheric temperatures higher at the poles, general circulation enhanced
- great quantities of water in the atmosphere (vapor and ice clouds) : 30 times more than present Mars (see 3.4).
- ice accumulation on the northern tropical zone, and on the southern zone (but less important). These two specific deposits tends to be permanent, and seems to be correlated with high-topography zones.
- water released from the permanent Northern cap does not return (it will take approx. 44,000 Earth years to completely exhaust this cap)

³Our results were presented during a workshop of two days at NASA Ames, featuring the NASA MGCM Team (Haberle, Montmessin, Hollingsworth, Colaprete, Schaeffer ...), Forget from LMD, France, but also an assembly of geologists (Carr, Head, Clifford, Kargel, Cabrol ...)

⁴figure 8, article [3]

⁵See 4.2 in the next chapter

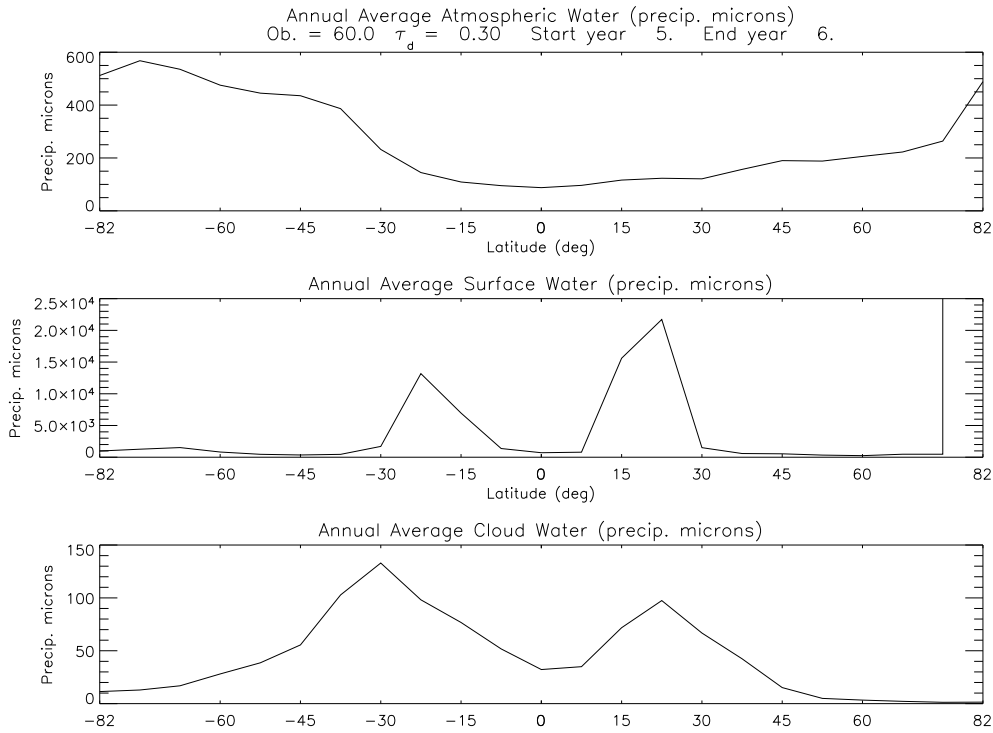


Figure 3.4: Annually and zonally averaged quantities of water vapor, surface ice, and ice clouds, as function of latitude. Simulation [noH]

3.2 Comparative simulations : 35° and 45° obliquity cases

3.2.1 Water cycle

The figure 3.5 shows the behavior of water reservoirs (vapor, ice clouds, ice ground) when we do simulations at 35° and 45°. Note that these simulations has not come to equilibrium in seven years. The plots of water vapor for example show that the water cycle in the south is not fully equilibrated from year to year in [o45] and [o35].

In [o35], all the quantities of water are lower than in [noH]. We still observe a peak of water vapor in the south, but the water cycle is a lot less active than in the 60° obliquity case. The water cycle slow down when the planet comes back to lower obliquity than 60°. It is much more sensitive to seasonal variations, and the quantities in precipitable microns involved are lower. The same plot than 3.4 gives an idea of the mean quantities : in [o35], annually and zonnally averaged, at few latitudes (mainly in South tropic), water vapor reaches no more than 100 $pr - \mu m$ (in [noH], it was 600 $pr - \mu m$), ice clouds 50 $pr - \mu m$ (150 $pr - \mu m$ in [noH]), and ground ice only 600 $pr - \mu m$ (compare to the nearly 20,000 $pr - \mu m$ in the [noH] case !). In [o45], we have water vapor 250 $pr - \mu m$, ice clouds 100 $pr - \mu m$, and ground ice 1200 $pr - \mu m$. In the 45° obliquity case, the water cycle is closer to what is happening in the 60° obliquity case, with lower quantities, especially in the North, more sensitive to obliquity changes.

3.2.2 Ground ice location

It is interesting to note that the behavior of the water vapor and ice clouds seems to be linear with the obliquity, but not the ice deposit. The behavior of ground ice seems much more sensitive to the obliquity than others parameters. We propose the idea that water vapor and ice clouds are not only quantities depending on the ground temperature balance between the pole and the equator, but also on atmospheric temperatures, which variations with obliquity are smoother than ground

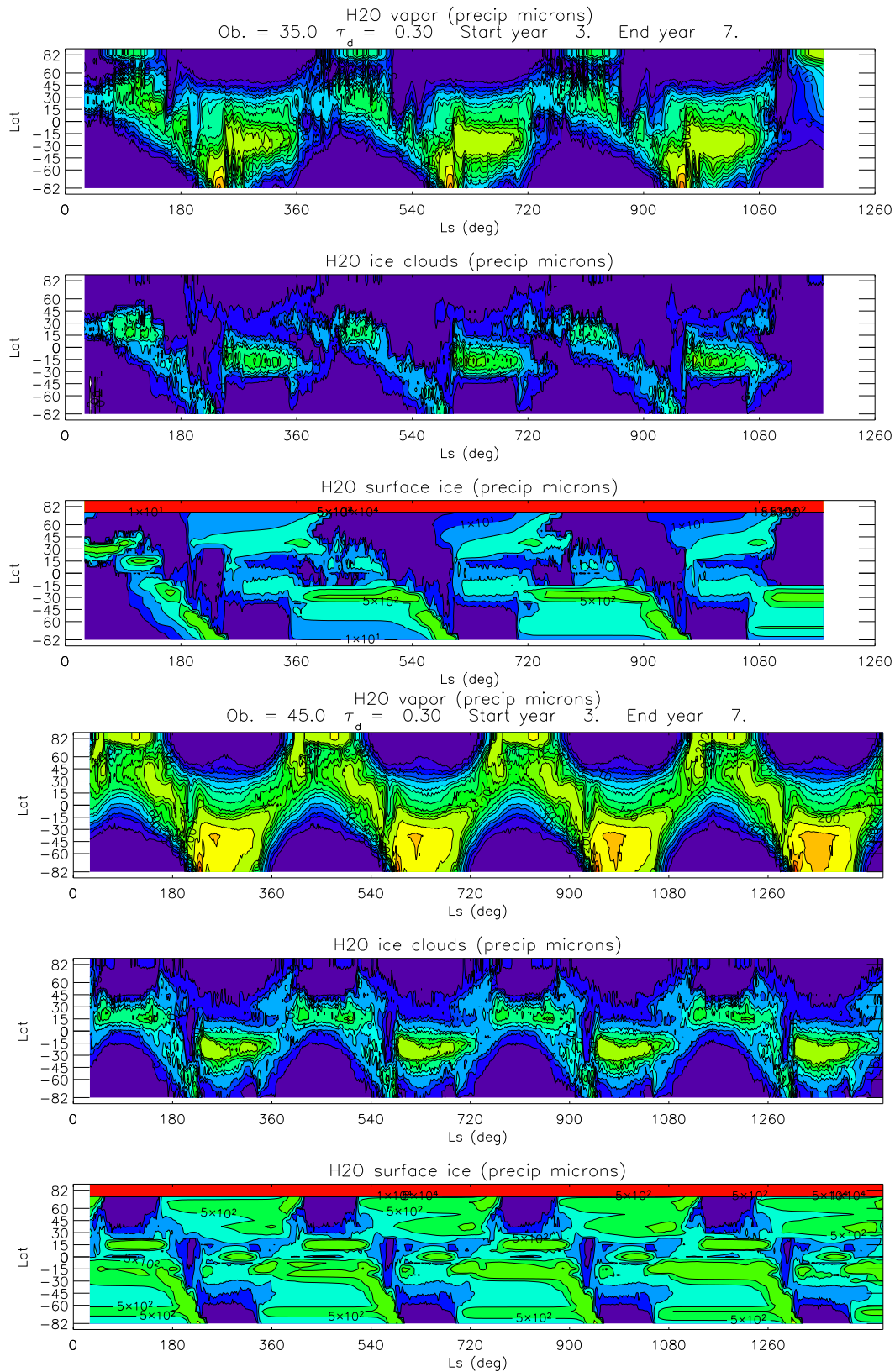


Figure 3.5: Summary of the water cycle behavior on the [o35] simulation (top three) and [o45] simulation (bottom three). Quantities in precipitable microns, as function of latitude and season, same color code as figure 2.8 and 3.1

temperature variations, because of the re-distribution of heat made by the general circulation. The ground ice location has something to do with the general circulation, but not the ground ice quantities, which depends quite exclusively of ground temperature. We have seen previously (figure 2.3) that the important threshold of obliquity was 54° (the poles receive more annual average insolation than the equator). This may account for the fact that when we change the obliquity from 35° to 45° , we see a linear increase of the ice deposition, but when we change the obliquity from 45° to 60° , the quantity of water ice ground deposition outside the North pole blow up.

We must also mention that this sudden explosion of ice deposition may be due to the fact that, in the [noH] case, the atmosphere is quite highly saturated, and the water vapor ratio is far above the water vapor saturation ratio - so a lot of ice starts to condensate from the great amount of water vapor in the atmosphere. This saturation is not reached in the [o35] [o45] case. However, the ground temperature argument we gave in the previous paragraph is still valid : we must remember that we see an explosion of water ground ice, but not an explosion of water clouds formation. So the saturation of the atmosphere shall not be the only explanation for such an exponential dependance of ice deposition with obliquity.

This striking difference between [o35]/[o45] and [noH] is reinforced if we look now at the stability of ice deposit. Figure 3.5 shows us no ice deposit that is stable annually, like we used to find on figure 3.1. With [o35], [o45], the plot 3.3 is dark blue all over the planet (except the North pole of course). Even the Tharsis ice deposit undergoes seasonal exhaustion. Only in the 60° obliquity case, the tropics latitudes become stable locations for ice accumulation.

However, ice is still taken from the North pole, and the result is still a net loss for the North pole, even if it is far from being as huge as [noH]⁶. But this water taken and spread over water reservoirs (vapor, clouds, ground ice) leads to no annually stable ice deposit. We plotted the same map than 3.3, but with the annually averaged quantity of water ice on the ground. This maps allows us to find where are the main seasonal places for ice deposition.

The maps 3.6 confirm that ice deposit is less important as the obliquity lowers from 60 to 45 and 35. There are also less distinct places of accumulation. The yellow-orange-red zones indicates places where ice deposit reach a value over 5 precipitable millimeters. Like in [noH], Tharsis is still a key location for ice deposit in [o45], as some places around Hellas crater, The difference we see between [o45] and [noH] is only the quantity of ice deposit and the annual stability, not the location. Even the places where few water ice is present seem to be quite the same in the two simulations. However, Elyseum Mons, in the North hemisphere, near longitude 180 is only a significant place where ice accumulates for the [noH] simulation. In [o35] we do not find any significant place for ice accumulation, except perhaps around Hellas crater.

We do not find in our simulations that the stable ice deposits move equatorward as the obliquity increases, like Mischna et al. found recently [13]. Let us emphasize that our simulations did not come to equilibrium, so we must be prudent, while comparing our results. Indeed, Mischna's team launched much longer simulations. Let us note also that the places for ice deposition they found are not exactly similar to ours - it seems that their model is more sensitive to thermal inertia variations and less sensitive to topography and circulation forcing.

3.2.3 General circulation

The intensity of the mass stream function is decreasing as the obliquity changes from 60 to 45 and 35. Of course, the mechanism involved is very complex, however, this change in the intensity of the general circulation is mainly due to the modification Mars' insolation, that cause changes in gradients of ground and atmospheric temperatures. In a very simple point of view, general circulation is driven by the contrasts between equator and pole. If we turn the obliquity of Mars to a higher value, we reinforce these contrasts, that is to say, gradients of temperature mainly. So it is no surprise to find

⁶It will take about 200,000 Earth years to exhaust the Northern water polar cap in the 45° obliquity case, and nearly 800,000 Earth years in the 35° obliquity case. These results however are not as reliable as the [noH] simulation, as equilibrium was not reached.

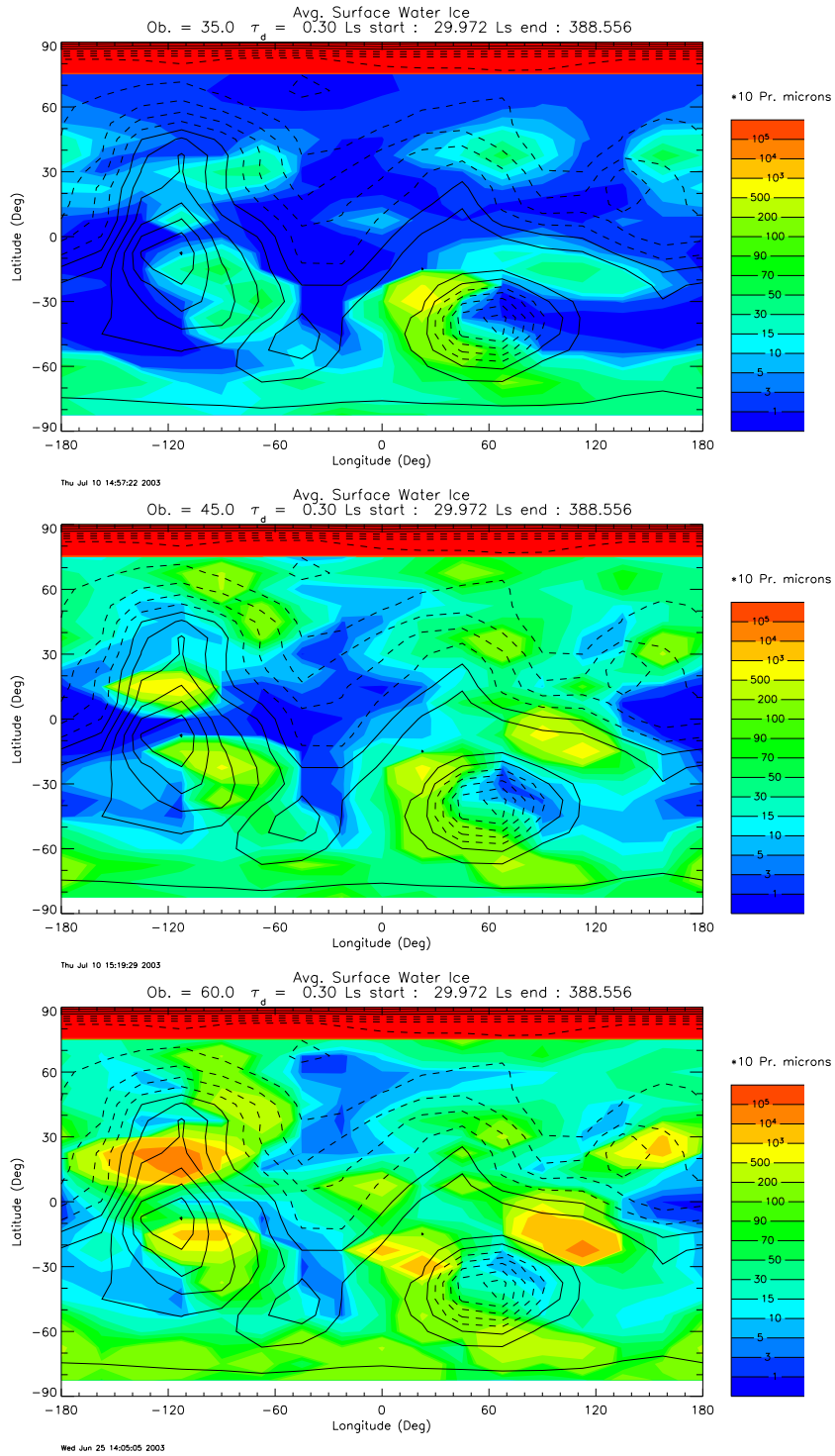


Figure 3.6: Averaged surface ice quantity, in precipitable microns, as function of latitude and longitude, from top to bottom : obliquity 35° [o35], obliquity 45° [o45], obliquity 60° [noH]

that the transport of mass throughout the planet slow down when the obliquity lowers from the high value of 60° .

3.2.4 Conclusion of the comparative study

We do not have to increase a lot the obliquity of Mars to obtain an enhancement of the water cycle, featuring increasing of all water reservoirs - vapor, ice clouds, ice ground. This enhancement is seen even in the 35° simulation. The climate is dominated by stronger temperature gradients and wider seasonal variations.

However, and it is an important conclusion of this study, annually stable ice ground may have occurred only when the obliquity of Mars undergo huge increasing to values near 60° obliquity. The places on the planet where it seems stable may have been preferentially high-topography zones.

The simulations we launched must be improved, but they are a good basis to start analyzing how could water ice deposits may have formed on Mars during obliquity cycles, and how generally speaking water may have been released from the polar sink where it is stuck in present-day Mars. Mars few thousands and millions years ago may have been a lot more wetter than today.

A lot of corrections can be brought to the conclusions we write here. For example, the model is now able to include the H_2O vapor radiative effect. Unfortunately, the clouds radiative effect is not ready to be simulated, like we mention previously.

Chapter 4

Simulations including the H_2O radiative effect

All the high-obliquity simulations done until now did not include the water vapor radiative effect. The simulations we launched are quite new. It was difficult for us to find some reference plots like we did for the previous chapter simulations.

There is a good reason for this lack of information. The GCMs have been designed for present-day Mars, where the amount of water vapor in the atmosphere is so small that the H_2O vapor radiative transfer can be reasonably neglected. The studies made at high obliquity use the same GCMs, whose radiative code was not adapted to take in account the radiative effect of such an amount of water vapor.

4.1 1D preliminary simulations

Our aim here is not to give a highly precise description of the radiative role of water vapor (see [1]). We saw in the first chapter that water vapor is too rare in the present Martian atmosphere to play a radiative role. However, at high obliquity, this role may be taken in account, especially the radiative transfer of water vapor in the infra-red. H_2O does not absorb a lot in the ultraviolet band of frequencies, but it does absorb and emit a lot in the IR frequency.

On Earth, this mechanism leads to some greenhouse effect : it is generally thought that water may be the predominant greenhouse gas on Earth. The molecules have some additionnal vibration-rotation energy given by absorption of IR photons emitted by the Earth surface. This energy is communicated to the whole atmosphere by collision with atmospheric molecules. Then the atmosphere can be a source of IR emission, in all directions, especially to the ground, where it warms the Earth surface. This IR emission slightly cool the atmosphere, because the energy absorbed by the atmosphere is used not for thermal agitation (what shall warm the atmosphere), but for thermal emission. We must admit this is very simplified way to see the IR radiative transfer of water vapor, but our aim is not to analyze precisely the effect of H_2O radiative effect. Even the radiative transfer equations are not fully understood, even if all the GCM include them.

The only specific study of the humidity role in the radiative transfer on Mars was done by Savijarvi [16], in 1991. The main difference between the two planets is that the direct radiative forcing of Mars' thin atmosphere is relatively stronger and more important than on Earth. Savijarvi did some 1D column simulations about the CO_2 radiative effect, adding at the end of his article the case of a "moist Mars". His conclusions were that "water vapour effects on the thermal radiation were found to be negligible in winter but not in summer. The daytime heating of the Martian lower atmosphere by absorption of solar radiation was very small regarding water vapor and weak as to CO_2 , when compared to the much stronger longwave daytime heating and nighttime cooling in a simulated summertime diurnal cycle".

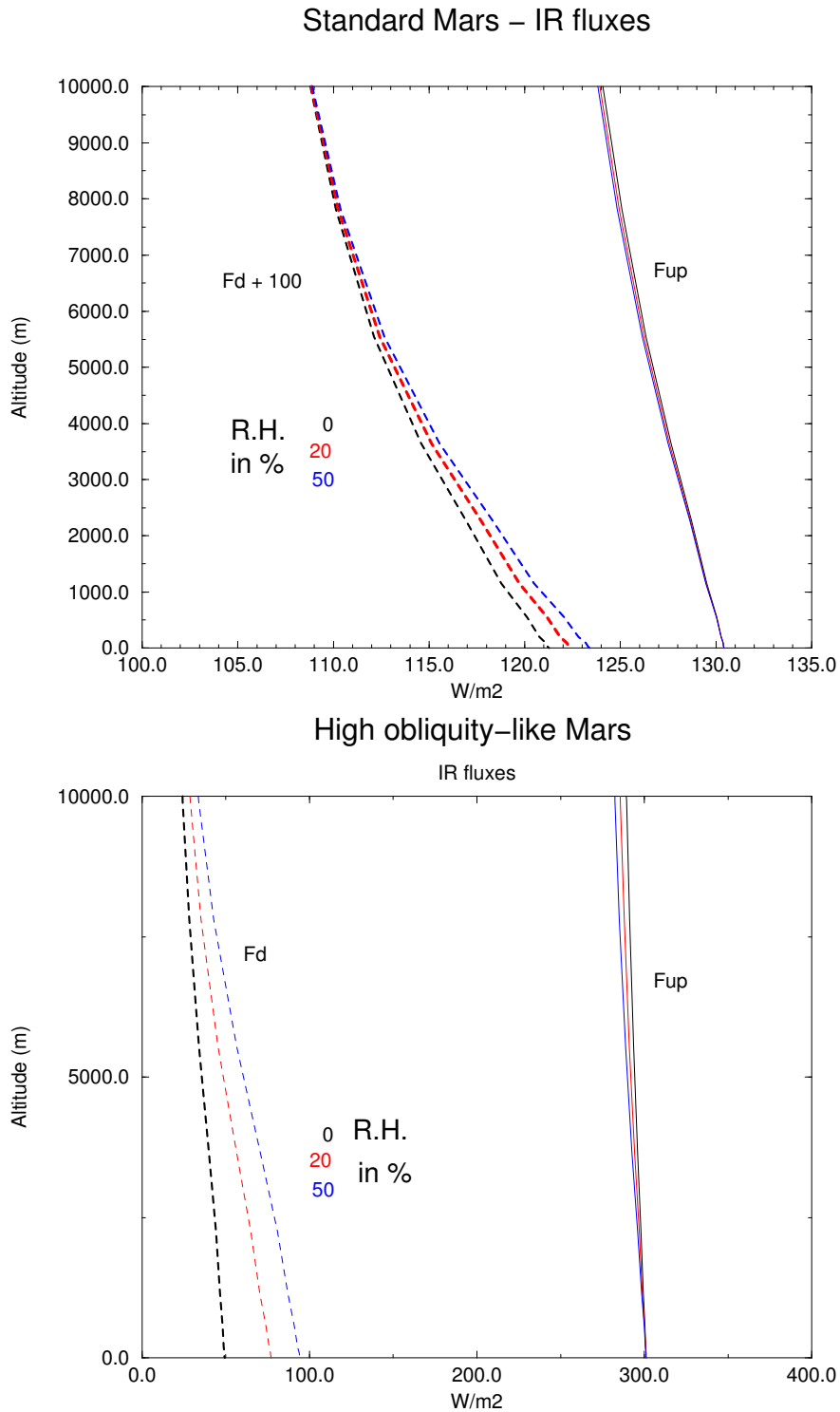


Figure 4.1: 1D instantaneous simulations of IR upward and downward fluxes [16]. Function of altitude

We are able to reproduce the simulations Savijarvi did¹, see figure 4.1. We strictly work on the same standard atmosphere profile Savijarvi used ($T_s = 219K$, $-\frac{dT}{dz} = 2.5K/km$, $p_s = 7mb$), and we try to work on the same kind of plot done in the figure 6, article [16]. We plot on 4.1 the downward and upward longwave fluxes, with relative humidity set at 0, 20 and 50%. The upward flux does not change much with increasing moisture amount as the extra absorption of the ground radiation to water vapor

¹Our model is even more precise

is compensated by increased emission from it. The downward flux increases with increasing moisture, especially near the surface. As a result, as relative humidity increases, there seems to be an extra greenhouse effect. Savijarvi concluded that such effects must be negligible during Martian winter, but probably not during Martian summer, where the moisture effects are enhanced. Consequently, we hope to see some greenhouse effect, in our simulations at high obliquity, where high amounts of water vapor are released in the atmosphere in the summers.

We plot also (bottom plot, 4.1) a "high-obliquity" case where we simply turn the surface temperature to his value at high obliquity at the poles, we choose the Northern pole, $T_s = 270K$. The extra greenhouse effect added by the water vapor in the atmosphere is enhanced. In the present-day case, note that the extra-greenhouse effect on the surface was $2W/m^2$ (10%) when relative humidity was increased from 0 to 50. On the bottom plot, we see that such an increase of humidity gives an extra-greenhouse effect of $50W/m^2$ (100%). This tends to show that the radiative effect of water vapor is very important on Mars at high obliquity.

4.2 Atmospheric behavior

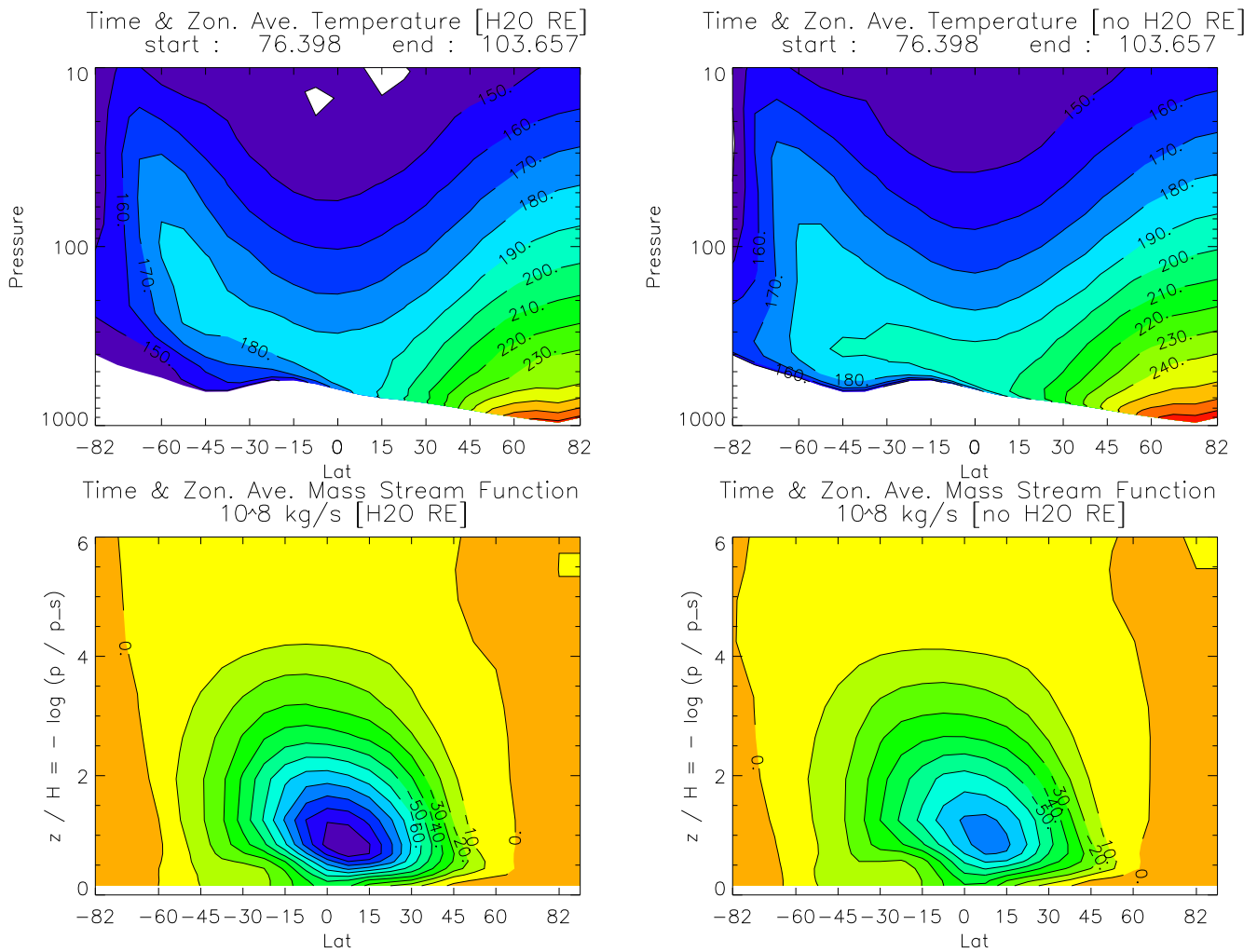


Figure 4.2: Northern summer atmospheric fields, in the [noH] (on the right) and the [H] (on the left) simulations, as function of latitude and pressure or pseudo-altitude. Zonally averaged atmospheric temperature on top and zonally averaged mass stream function on bottom. These quantities are averaged on a time interval around $L_s = 90^\circ$.

Firstly, we would like to mention the behavior of the ground temperature when we turn on the radiative effect of water vapor. What we see is logically (see previous section) a greenhouse effect that tends to warm the surface - however, this extra-greenhouse effect (2 to 3 K increase of the ground temperature) happens only at the poles on their respective summer. The map we plotted, showing the difference for ground temperature in [noH] and in [H], as function of latitude and season, is quite similar to the water vapor map (see 2.8).

Secondly, as developed in figure 4.2 (Northern summer). the atmospheric behavior at the solstices is very sensitive to the addition of the water vapor radiative effect. We observe a strong cooling of the atmosphere, nearly 30 K in the lowest part of the atmosphere in the South between latitude -45 and -60, and about 10 K in the lowest part of the atmosphere in the North between latitude 45 and 60. In the southern summer, we see the same effect, but in the two hemispheres the cooling reaches only 10 K. In the equinoxes, differences are quite low, and not significant. In figure 4.2, we also see a strong modification of the gradients : vertically, gradients are smoother (compare at latitude -45), and horizontally, as we mentioned earlier, there is an increasing of the contrast between North and South pole.

The bottom plots show that the Hadley cell intensifies, as we turn on the radiative effect of water vapor. This is very puzzling, because we thought that the cooling of the atmosphere was basically a consequence of a smoother circulation, but this is not the case. We have to explain how the general circulation can intensify, as the atmosphere is cooler. Circulation is driven by differential heating - pole to pole contrast². We mentioned above, that, in addition to the atmospheric cooling, there is an intensification of the pole to pole gradient. Providing this argument, the enhancement of the Hadley cell seems logical. Nevertheless, an intensification of the Hadley cell seems far from being consistent with a cooling of the atmosphere. One thing is certain, the radiative effect of water vapor only can not account for such an atmospheric cooling, there may be other influences. The plot 4.2 is still for us quite a mystery - we surely lack a more accurate study of the interactions between temperature profile and mass stream function.

4.3 Water cycle behaviour

It is worth starting our discussion remarking that turning on the H_2O radiative effect caused no instability in the GCM. Moreover, we can consider the water cycle as correctly simulated. The intervention of H_2O as a radiative agent does not seem to modify dramatically the general water cycle seen formerly. The plots are similar to the previous plots 2.8 and 3.1, the differences seen are for example the values of seasonal peaks. We can say that the general water cycle is not modified when we turn on the water vapor radiative effect.

The water cycle stabilizes a little bit slowly as previously - that is to say, within four years, instead of three years. However, we will consider as reliable a comparison based on the sixth year of each simulation. The plot 3.4 was summarizing quite well the quantities playing a role in the water cycle - so we did a plot where we made a difference between the [H] results and the [noH] results (see 4.3).

Here are the conclusions we propose :

- More water ice is taken from the North Ice Polar Cap
- More water vapor is found in the Southern and the Northern high-latitudes. Less water vapor is found in the equatorial region.
- More water ice clouds are created - and the same tendency is followed by both hemispheres.
- Same amount of water ice is falling on the ground in the Southern hemisphere, however, the ice deposit in the Northern hemisphere is done in greater quantities than [noH], and extends to latitude [30-45] (in the [noH] case the ice deposits were between latitude [-30,30]).

²pole to equator for Earth

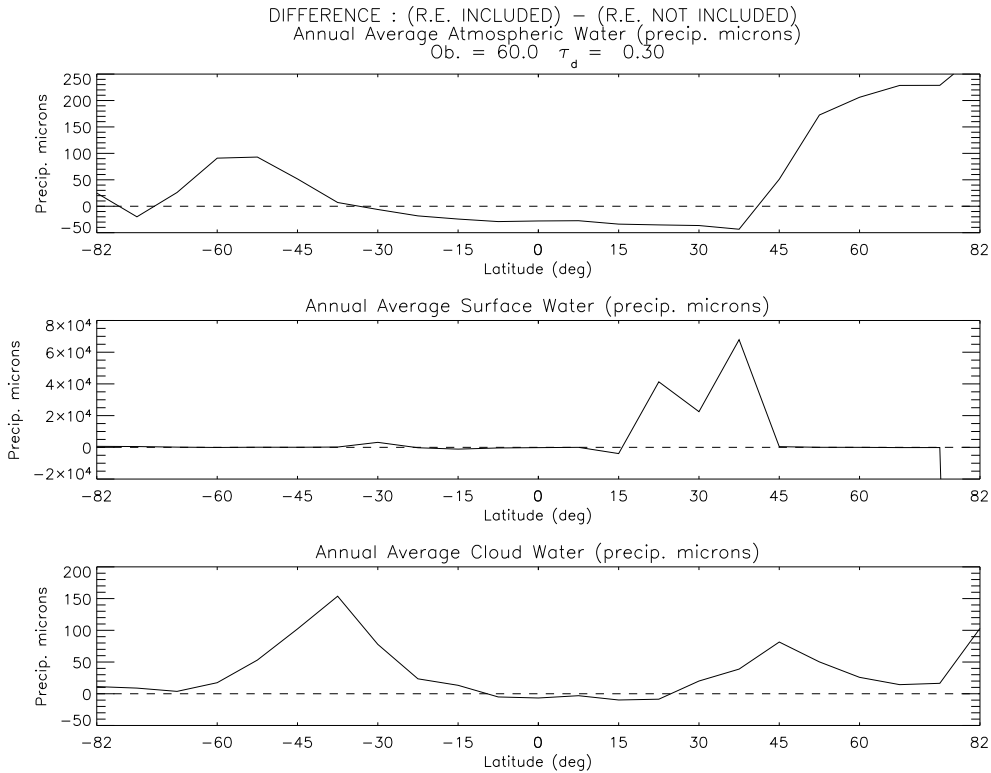


Figure 4.3: Annually and zonally averaged quantities of water vapor, surface ice, and ice clouds, as function of latitude. Simulation [H] - simulation [noH], dash line is zero

There are two opposite mechanisms in competition :

1. The atmosphere at the poles in summer is cooler (difference of 10 K between [H] and [noH]), which means a decrease of the maximum atmospheric holding capacity of water (see Thermodynamics in the first chapter).
2. The surface temperature at the poles on their respective summer is warmer, of about 3K, due to the greenhouse effect of water vapor, so the water vapor released in the atmosphere is likely to increase. If we increase T_{surf} , we will have P_{sat} increasing at the surface, and then more water vapor will be sublimated.

The effect (2) predominates at the poles, that is why more water vapor is found there. However, at the equator, the effect (1) is stronger than effect (2) (no increase of ground temperature near the equator), So the atmosphere, very close to saturation, can hold less water vapor in the equator, in comparison with the [noH] simulation. That is what is observed in figure 4.3. This could also be a consequence of the enhanced general circulation at the solstices.

We would like to mention that all the tendencies seen undergo a positive feedback. For example, at the Northern pole, during summer, more water vapor is released in the atmosphere, due to the extra-greenhouse effect of water vapor at the poles - this water vapor added in the atmosphere is a guarantee that the greenhouse effect is self-induced, so the feedback is positive.

In addition, in the mid-latitudes, the effect (1) is still stronger than effect (2) (the H_2O greenhouse effect is really concentrated at the poles), so as the atmosphere cannot hold as much water vapor as previously in the [noH] case, this vapor condensates in water ice and creates at new deposit on the ground. It is interesting to note that no additional deposit is found in the South, but if we glance at the ground temperature differences map, we see that in the South, the greenhouse effect is extended to -45 latitude, unlike the North hemisphere, where significant greenhouse effect is only very close to

the pole. This fact explains the mid-latitude asymmetry between North and South observed in the middle plot in figure 4.3.

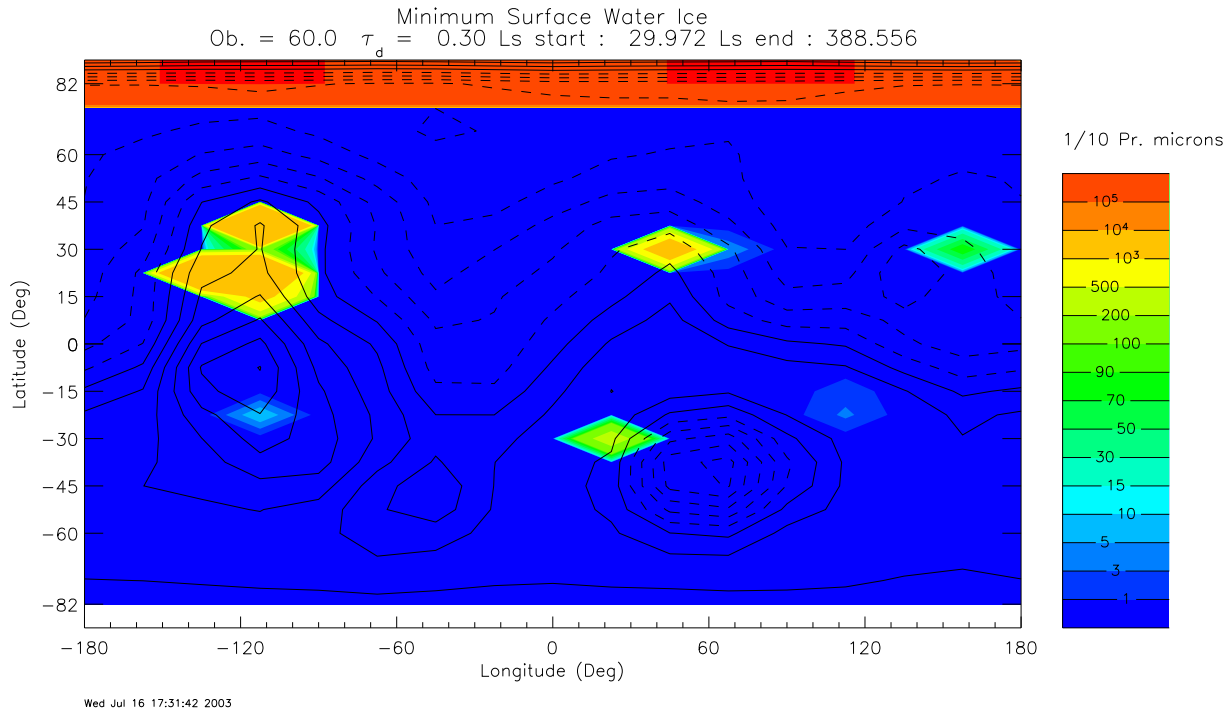


Figure 4.4: Latitude/longitude plot, simulation [noH]. Annual minimum of water ice ground, in precipitable microns. Dark blue means zero.

This new deposit can be seen in 4.4, same kind of picture as 3.3. The Alba Patera high plateau become a stable destination for ice deposit. Another place for stable ice can also be found in the Northern hemisphere, in a zone of topography gradient. Note that in the Southern hemisphere, the deposit near Hellas is not at the same place as [noH]. This slight shift in the location of ice deposits tends to show that places where ice accumulates are very sensitive to any change of the simulation conditions. We can guess that if we include the cloud radiative effect, there will also be some modifications. However, Tharsis still seems to be a key location for stable water ice deposit throughout the Martian year.

We make the same calculation than we did in [noH], about how many years need the Northern polar cap to fully exhaust. The result is 18,000 Earth years, about twice less than the simulation [noH]. This result is interesting, because it means that once the process of acceleration of the water cycle have begun at high obliquity, rapidly there will be great amounts of water vapor in the atmosphere, and then, H_2O vapor will be regarded as significant, radiatively speaking. Eventually, the exhaustion of Northern water polar cap will accelerate. Finally, we find here that the 44,000 year exhaustion time we had previously is over-estimated.

4.4 Conclusion

About the meteorological fields :

- Atmosphere cooler (about 10 K) -> decrease of the holding capacity in water
- Surface warmer at the poles on their respective summer (about 3 K) -> slight increase of the sublimation rates
- General circulation stronger -> is it consistent with the cooling of the atmosphere ?

About the water reservoirs :

- More water vapor, except at the low latitudes.
- More ice clouds.
- More ground ice, and wider repartition on the planet. Alba Patera becomes a destination for ground ice.
- Accelerated exhaustion of the Northern polar cap

These results are still not complete, as the radiative effect of water ice clouds still need to be included in the model.

Chapter 5

Conclusions : Abstract

The short abstract (see next two pages) summarizes the main conclusions of our work, that are supposed to be presented during the Mars Polar conference.

We have obtained some great results, even if there are still a lot of work to be done. However, the efforts made until now have led us to get very promising results for the description of paleo-climates of Mars at high obliquity.

Finally, here are some improvements that could be done to the study we started :

- simulate the radiative effect of water ice clouds
- try to put initial source of water in other places than the Northern cap
- analyze the effects of dust storms
- make longer simulations, with a better resolution

Acknowledgements

I would like to thank Bob Haberle, Franck Montmessin, Francois Forget, James Schaeffer, Jeffery Hollingworth, and Antony Colaprete. A special thanks for Franck, who was always here to help me, and for Bob, who was from the first day very welcoming with me, and give me, with Francois and Franck, a chance to do my best to participate to their present researches.

This internship was a wonderful and unforgettable experience. It was an opportunity to see interesting and motivating applications of the theories I learnt at Ecole Polytechnique, in the majeure Planete Terre. It was a first, and very satisfying, experience in the world of research, where I improved my computer and English skills, my scientific reflexion, and my ability to adapt quickly. The presentation I did at the workshop was also a useful experience.

OBLIQUITY DRIVEN CLIMATE CHANGE IN MARS' RECENT PAST. R.M. Haberle¹, F. Montmessin¹, F. Forget², A. Spiga³, and A. Colaprete⁴. ¹Space Science Division, MS 245-3, NASA/Ames Research Center, Moffett Field CA, 94035, Robert.M.Haberle@nasa.gov. ²Laboratoire de Météorologie Dynamique, Université Paris, 4 pl. Jussieu, 75252 Paris Cedex 05-FRANCE, forget@lmd.jussieu.fr. ³École Polytechnique, 91128 Palaiseau, Cedex FRANCE, Aymeric.Spiga@polytechnique.org. ⁴SETI Institute, Space Science Division, MS 245-3, NASA/Ames Research Center, Moffett Field CA, 94035, tonyc@freeze.atc.nasa.gov.

Introduction: To explain the equatorial valley networks on Mars, Jakosky and Carr [1] suggested that water ice now stored in the north polar region would be mobilized at high obliquity and precipitate out at low latitudes. Extrapolating the present day latitudinal distribution of water vapor to high obliquity conditions, and noting that the low latitude atmosphere would be saturated, they predicted substantial surface ice deposits would accumulate in the tropics at such times.

The first general circulation model simulations to verify this prediction were reported by Haberle et al. [2] who found that while ice can accumulate at low latitudes at high obliquity, it is distributed regionally depending on orbital conditions. Forget [3], Richardson and Wilson [4], and Mischna et al. [5], subsequently obtained similar results with independent models. Thus, obliquity driven climate change may help explain the many tropical landforms thought to be sculpted by water in one form or another (see, for example, refs [6], [7], and [8]).

While low latitude ice accumulations at high obliquity appears to be a robust result, the major challenge now facing models is predicting ice accumulations in the same places where the geological evidence suggests it occurred. This will depend not only on orbital conditions, but also on what physical processes the models include in the hydrological cycle. For example, none of the models mentioned above include the radiative effects of water vapor or clouds, yet both are expected to be in abundance at high obliquity. And none of the models has a very realistic cloud microphysics scheme, which can have a significant effect on how clouds affect the planet's radiation balance.

Here we extend these early modeling results by including a more sophisticated cloud microphysics package, as well as the radiative effects of water vapor and clouds.

Model description: We use the NASA/Ames C-grid Mars general circulation model with an updated radiation code and cloud microphysics scheme. To speed up the simulations, we run the model at fairly coarse resolution (7.5° latitude \times 22.5° longitude). Future efforts will examine the effect of resolution on the results.

Radiation Code Fluxes and heating rates are calculated from a radiation code based on the two-stream solution to radiative transfer that fully accounts for multiple scattering in the presence of gaseous absorption. The model has 12 spectral intervals. Dust and water ice scattering properties are included. For dust, we use the Ockert-Bell [9] values in the visible, and Forget [10] values in the infrared. For ice, we can either compute them online as the cloud evolves, or we can specify them. Gaseous opacities for water vapor and CO₂ are calculated from correlated k-distributions taken from full line-by-line models.

Cloud Microphysics Our cloud scheme is based on a moment/oider scheme in which the mass mixing ratio and number density of the cloud ensemble are the advected species. From these we obtain a mean particle size and an estimate of the particle size distribution (assuming a variance) which we then divide into 8 bins. Cloud microphysics is performed in each of these bins and includes nucleation, condensation, and gravitational settling. Dust is treated as a tracer and serves as condensation nuclei. The advected size distribution is then converted back into a mean size, a mixing ratio, and a particle number density.

Results: We have conducted simulations for a variety of different obliquities, all at present solar luminosity. In each case the model is spun up from dry initial conditions with a residual ice cap at the north pole. After several years, depending on obliquity, the atmosphere equilibrates and repeats from year-to-year. A sample result for the 60° obliquity simulation, without the radiative effects of clouds or water vapor, is shown in Fig. 1. The top panel in Fig. 1 is the zonally averaged column water vapor as a function of time for 7 Mars years. The middle and bottom panels are similar, but for cloud mass and surface ice, respectively.

Water ice subliming from the north residual cap during summer is rapidly transported southward. Clouds form in low northern latitudes and ice precipitates to the surface. The remainder is transported into the southern hemisphere and condenses onto the south seasonal CO₂ ice cap which extends almost to the equator at the solstice. When the south cap retreats, water is released into the atmosphere where some precipitates back to the surface and the remainder is transported north. Again clouds form in the low latitudes

and ice precipitates to the surface. At equilibrium, thousands of precipitable microns of water vapor appear in the summer polar regions. There is more water in the south than the north because the south cap is a better trap for water, and because the Southern Hemisphere is warmer during summer than in the north. Cloud abundances also reach the thousand precipitable micron mark with model predicted particle sizes in the 20-30 micron range. These particles are much bigger, and subsequently fall out faster, than those for present obliquity.

Eventually, permanent deposits form (i.e., ice remains on the ground all year long) in the low latitudes of each hemisphere. These deposits are concentrated along the northern flanks of the Tharsis region and to the northeast of the Hellas basin. Topography plays a key role on where the deposits form through its influence on the circulation. The deposits do not necessarily form in locations where the mean annual surface temperatures are a minimum. They form where the saturation state of the atmosphere is highest. This, in turn, is influenced not only by the thermal structure of the atmosphere, but also by the transport characteristics of the atmosphere.

Simulations which include the radiative effects of water vapor show similar results, but with (a) an increase in the amount of surface ice, (b) a slight shift in the location of the deposits, (c) a cooler and cloudier atmosphere, and (d) slightly warmer surface temperatures. We are presently undertaking simulations with the radiative effects of clouds included and will report the results at the meeting. However, off line 1-D simulations using the predicted cloud abundances indicate they will have a much greater influence on the results than water vapor alone. Their abundances (~1000 μm), particle sizes (20-30 μm), widespread occurrence, and impact on the solar and infrared radiation fluxes give clouds a much greater role in determining the climate at high obliquity than for present day conditions.

Conclusions: Mars has a natural mechanism for experiencing significant climate change and redistributing surface ice. Obliquity changes alone are quite capable of moving ice into low latitudes and may provide an explanation for the many geological landforms that strongly indicate recent climate change.

References: [1] Jakosky, B.M. and Carr, H.H. (1985) *Nature*, 315, 559-561. [2] Haberle, R.M., et al. (2000) *LPS XXXI*, Abstract #1509. [3] F. Forget (2001), personal communication. [4] Richardson, M.L., and Wilson R.J., *JGR*, 107, 5031-5049. [5] Mischka, et al. (2003) *JGR*, In press. [6] Cabrol, N.A. and Grin, E.A. (2001). *Icarus*, 149, 291-328. [7] Kasting, J. (2001) DPS Abstract # 48.12. [8] Head, J.W. and Mar-

chant, D.R. (2003) 6th International Mars Conference, Abstract #3807. [9] Ockert-Bell, M.E. et al. (1997). *JGR*, 102, 9039-9050. [10] Forget, F. (1998). *GRL*, 25, 1105-1108.

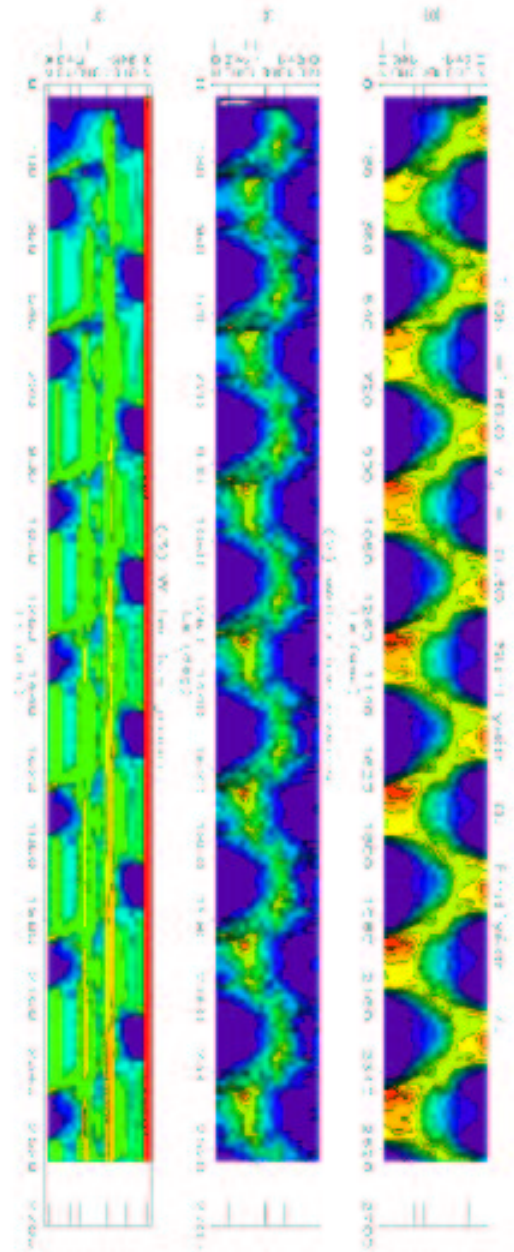


Figure 1

Bibliography

- [1] Chassefiere E., Amiranoff F., Pillet P. (1999) Physique de l'atmosphere et methodologies d'observation, Cours de l'Ecole Polytechnique
- [2] Forget F. (1996) Le climat de la planete Mars : de l'importance des poussieres et des regions polaires, These de Doctorat de l'universite Paris 6
- [3] Forget F., Hourdin F. et al. (1999) Improved general circulation models of the martian atmosphere from the surface to above 80 km (section 9), JGR - Planet, vol 104
- [4] Haberle R.M., Pollack J.B., Barnes J.R., Zurek R.W., Leovy C.B., Murphy J.R., Lee H., Schaeffer J. (1993) Mars atmospheric dynamics as simulated by the NASA Ames general circulation model 1-The zonal mean circulation, JGR, vol 98, 3093-3123
- [5] Haberle R.M., Joshi M.M., Murphy J.R., Barnes J.R., Schofield J.T., Wilson G., Lopez-Valverde M., Hollingsworth J.L, Bridger A.F.C., Schaeffer J. (1999) General circulation model simulations of the Mars Pathfinder atmospheric structure investigation/meteorology data, JGR, vol 104, 8957-8974
- [6] Haberle R.M. (2001) Planetary Atmospheres/Mars
- [7] Haberle R.M., Murphy J.R., Schaeffer J. (2003) Orbital change experiments with a Mars general circulation model, Icarus 161, 66-89
- [8] Jakovsky B.M., Carr M.H. (1985) Possible precipitation of ice at low latitudes of Mars during periods of high obliquity, Nature, 315, 559-561
- [9] Jakovsky B.M., Haberle R.M. (1992) The seasonal behavior of water on Mars, chapter 28, p 969-1016, University of Arizona Press
- [10] Kieffer H.H., Zent A.P. (1992) Quasi-periodic climate change on Mars, *Mars*, chapter 33, p 1181-1218, University of Arizona Press
- [11] Laskar J., Robutel P. (1993) The chaotic obliquity of the planets, Nature 361, 608-612
- [12] Le Treut H., Bougeault P. (2003) Dynamique de l'atmosphere et des oceans, Cours de l'Ecole Polytechnique
- [13] Mischna M.A., Richardson M.I., Wilson R.J., McCleese D.J. (2003) On the orbital forcing of Martian water and CO₂ cycles : a general circulation model study with simplified volatile schemes, JGR, vol 108, article in press
- [14] Montmessin F. (2002) Aspects microphysiques de l'atmosphere martienne : du role des nuages et des poussieres, These de Doctorat de l'universite Paris 6
- [15] Richardson M.I., Wilson R.J. (2002) Investigation of the nature and stability of the Martian seasonal water cycle with a general circulation model, JGR, vol 107, E5

- [16] Savijarvi H. (1991) Radiative fluxes on a dustfree Mars, Beitr. Phys. Atmosph., vol 64, no 2, p. 103-112
- [17] Toon O.B., Pollack J.B., Ward W., Burns J.A., Bilski K. (1980) The astronomical theory of climatic change on Mars, Icarus 44, 552-607
- [18] Zurek R.W., Barnes J.R., Haberle R.M., Pollack J.B., Tillman J.E., Leovy C.B. (1992) Dynamics of the Atmosphere of Mars, *Mars*, chapter 26, p 835-933, University of Arizona Press